

Phenomenological study of hadron interaction models

H.R. Pang¹, J.L. Ping², Fan Wang¹ and T.Goldman³

¹*Physics Department, Nanjing University, Nanjing, 210093, China*

²*Physics Department, Nanjing normal University, Nanjing, 210097, China*

³*Theoretical Division, LANL, Los Alamos, NM 87545, USA*

Abstract

We present a phenomenological study of three models with different effective degrees of freedom: a Goldstone Boson Exchange (GBE) model which is based on quark-meson couplings, the quark delocalization, color screening model (QDCSM) which is based on quark-gluon couplings with delocalized quark wavefunctions, and the Fujiwara-Nijmegen (FN) mixed model which includes both quark-meson and quark-gluon couplings. We find that for roughly two-thirds of 64 states consisting of pairs of octet and decuplet baryons, the three models predict similar effective baryon-baryon interactions. This suggests that the three very different models, based on different effective degrees of freedom, are nonetheless all compatible with respect to baryon spectra and baryon-baryon interactions. We also discuss the differences between the three models and their separate characteristics.

PACS numbers: 12.39.-x, 14.20.Pt, 13.75.Cs, 13.75.Ev

I. INTRODUCTION

Hadronic interactions are central to strong interaction physics. However, for the time being, the fundamental strong interaction theory, Quantum ChromoDynamics (QCD) remains too complicated for these to be directly calculated from it. Nevertheless, initial lattice QCD calculations of hadronic interactions [1] have been initiated. Due to the complication of a multiquark system, however, quantitative results remain in the distant future.

Meson exchange models, based on meson-baryon couplings, were developed long before QCD [2] and are still the best at fitting the vast collection of NN experimental data [3]. Unfortunately, the QCD basis for such effective degrees of freedom in *t-channel* exchanges is not clear at present. Chiral perturbation effective field theory [4] is well-based in QCD; for a recent derivation, see [5]. However, due to the fact that the quark and gluon degrees of freedom have been integrated out, it can not be used to study the quark-gluon internal structure of hadrons. Nor is it suitable for the study of genuine multiquark-gluon systems such as glueballs, hybrids, $q\bar{q}q\bar{q}$ systems, and dibaryons.

R.T.Cahill et al. [6] have developed an effective field theory which takes spontaneous chiral symmetry breaking into account. Constituent quarks and Goldstone bosons appear here as the effective degrees of freedom for low energy QCD physics. This model has been applied both to pion and σ meson internal structure and to meson interactions, but not yet to NN interactions [7]. L.Ya.Glozman, D.O.Riska and G.E.Brown [8] propose a phenomenological model, with constituent quarks and Goldstone bosons as the effective degrees of freedom for describing baryon spectroscopy and baryon interactions. However, their quark meson coupling is the linear Yukawa coupling, which reflects neither QCD based chiral perturbation nor the nonlinear coupling obtained from the effective field theory referred to above.

A.Manohar and H.Georgi [9] have argued that below the chiral symmetry breaking scale ($\sim 1\text{Gev}$) and within the confinement regime ($\sim 1\text{fm}$), the proper effective degrees of freedom are Goldstone bosons, constituent quarks and gluons. (We have constructed an approximate QCD derivation of this model, similar to Cahill's approach, but the quantum

fluctuations of the gluon field are suppressed.) Such a hybrid quark-gluon-meson exchange model has been widely used to describe nucleon-baryon interactions and a semi-quantitative fit has been obtained [10].

Models with constituent quarks and effective one gluon exchange [11] describe hadron spectroscopy quite well. The Hamiltonian approach to QCD [12] seeks the QCD basis for this model. The Schwinger-Dyson equation approach also keeps constituent quarks and gluons as the effective degrees of freedom [13]. However, direct extension of this model to the NN interaction obtains only a repulsive core [14]. A variant of this model obtains the NN repulsive core and intermediate range attraction simultaneously, by taking into account both quark delocalization and color screening. This also describes a qualitative similarity between nuclear and molecular forces. A semiquantitative fit to the existing NN, NA, and N Σ scattering data and to properties of the deuteron has been obtained as well [15].

The MIT bag model uses current quarks and gluons to describe hadron internal structure [16]. A quark-meson coupling has to be introduced to restore chiral symmetry [17] to this model; Cahill et al. have given an approximate QCD derivation [6]. The model has been extended to the description of hadron interactions using the R-matrix method and compound quark model approach [18].

The Skyrmion model can be viewed as originating from the large N_c limit. It has been used both for nucleon internal structure and for hadronic interactions [19]. The nontopological soliton model also acquired an approximate QCD derivation a few years ago [20].

There might be even more QCD models that can be listed. But this short review suggests that neither theoretical studies of QCD nor phenomenological model analyses can yet determine which effective degrees of freedom are best, nor which model is best for the description of low energy hadron physics. Therefore, theoretical study of QCD and phenomenological analysis are both still needed to extend our understanding of low energy strong interaction physics.

This paper reports a phenomenological study of the effective baryon-baryon interactions of the ground state octet and decuplet baryons using three constituent quark models with

quark-meson, quark-meson-gluon, and quark-gluon effective degrees of freedom respectively. The results show that in many channels, (about 2/3 of the total states) the three different models give more or less the same predictions. We take this as a phenomenological verification that, even for baryon-baryon interactions, quark models with different effective degrees of freedom are quite compatible and that meson exchange effects are modeled, at least to some extent, by quark delocalization and color screening. In some channels, however, especially promising dibaryon states, the different models give drastically different predictions. These cannot be viewed as being as reliable as those above; i.e., these results are sensitive to model details. Experimental searches in those channels are needed to distinguish the validity of the different models.

This paper is organized as follows: In Sec. II, we describe the Hamiltonians and parameters of the three models. In Sec. III, we present the results and discuss them. The final section gives our conclusions.

II. HAMILTONIAN AND PARAMETERS OF THREE MODELS

From among the models discussed in the introduction, we choose three constituent quark models on which to do a comparative phenomenological study; i.e., we calculate the adiabatic effective baryon-baryon interactions and dibaryon candidates systematically. The three models are: the Glozman-Riska-Brown model, based on constituent quarks and exchange of Goldstone bosons (GBE); the Fujiwara model, based on constituent quarks and gluons, with the Nijmegen description of one boson exchange (FN); the quark delocalization and color screening model (QDCSM), based on constituent quarks and gluons but with quark delocalization and color screening effects included. We choose to consider these three models for several reasons: There has been considerable debate recently regarding these effective degrees of freedom [21]; These models have been extensively studied with respect to baryon spectroscopy and baryon-baryon interactions; They can be calculated straightforwardly in a consistent, systematic way, using fractional parentage expansions and variational methods.

A. Quark and meson effective degrees of freedom: GBE models

We take the Goldstone Boson Exchange (GBE) model of Glozman's group as the example with constituent quarks and Goldstone bosons as the effective degrees of freedom. This model has been successfully applied to baryon spectra and also extended to study NN interactions. Although recent research shows that scalar and vector mesons should also be included to describe baryon-baryon interactions, here we use only the original version, i.e., only pseudo-scalar mesons (as Goldstone bosons), which gives a surprisingly good description of baryonic spectra.

In the nonrelativistic meson-exchange quark-quark interaction of any such model, there is a δ -function term, which is true only for point-like particles. For particles with structure, this δ -function must be smeared out. In the GBE model, two types of smearing were used: Gaussian and Yukawa. We designate them as model GBE(a) and GBE(b), respectively.

1. GBE with Gaussian smearing: GBE(a)

In this case, the δ -function is smeared by a Gaussian function [22]. This version provides a successful description of the spectroscopy of baryons. In addition, the short-range repulsion of the NN interaction is also obtained. This Gaussian smearing involves two parameters corresponding to the short range cutoff point (r_0) and the width (α) of a bell-shaped curve.

$$\begin{aligned}
 H &= \sum_i m_i + \sum_i \frac{P_i^2}{2m_i} - \frac{(\sum_i P_i)^2}{2\sum_i m_i} + \sum_{i<j} V_{conf}(r_{ij}) + \sum_{i<j} V_\chi(r_{ij}) \\
 V_{conf}(r_{ij}) &= -\frac{3}{8}\lambda_i^c \cdot \lambda_j^c (Cr_{ij} + V_0) \\
 V_\chi(r_{ij}) &= \left\{ \sum_{F=1}^3 V_\pi(r_{ij})\lambda_i^F \cdot \lambda_j^F + \sum_{F=4}^7 V_k(r_{ij})\lambda_i^F \cdot \lambda_j^F + V_\eta(r_{ij})\lambda_i^8 \cdot \lambda_j^8 + V_{\eta'}(r_{ij})\lambda_i^0 \cdot \lambda_j^0 \right\} \sigma_i \cdot \sigma_j \\
 V_\gamma(r) &= \frac{g_\gamma^2}{4\pi} \frac{1}{12m_i m_j} \left\{ \theta(r - r_0) \mu_\gamma^2 \frac{e^{-\mu_\gamma r}}{r} - \frac{4}{\sqrt{\pi}} \alpha^3 \exp(-\alpha^2(r - r_0)^2) \right\} \\
 \gamma &= \pi, k, \eta, \eta'
 \end{aligned}$$

where the parameters are

$$\mu_\pi = 139MeV, \mu_k = 495MeV, \mu_\eta = 547MeV, \mu_{\eta'} = 958MeV$$

$$m_{u,d} = 340MeV, m_s = 440MeV, \frac{g_{\pi q}^2}{4\pi} = \frac{g_{\eta q}^2}{4\pi} = \frac{g_{kq}^2}{4\pi} = 0.67$$

$$\frac{g_{\eta' q}^2}{4\pi} = 1.206, r_0 = 0.43fm, \alpha = 2.91fm^{-1}, V_0 = 0, C = 0.474fm^{-2}, b = 0.437fm.$$

Here b is the baryon size parameter (a parameter of the quark orbital Gaussian wave function).

2. GBE with Yukawa smearing: GBE(b)

Because Gaussian smearing does not meet the well known requirement that the volume integral of the pseudoscalar meson exchange interaction should vanish, another smearing version, Yukawa smearing, was also applied in the GBE model [23].

$$V_\gamma(r) = \frac{g_\gamma^2}{4\pi} \frac{1}{12m_i m_j} \left(\mu_\gamma^2 \frac{e^{-\mu_\gamma r}}{r} - \Lambda_\gamma^2 \frac{e^{-\Lambda_\gamma r}}{r} \right), \Lambda_\gamma = \Lambda_0 + \kappa \mu_\gamma$$

$$m_{u,d} = 340MeV, m_s = 507MeV, C = 0.77fm^{-2},$$

$$\frac{g_{\pi q}^2}{4\pi} = \frac{g_{Kq}^2}{4\pi} = \frac{g_{\eta q}^2}{4\pi} = 1.24, \quad \frac{g_{\eta' q}^2}{4\pi} = 2.7652, \Lambda_0 = 5.82fm^{-1}, \kappa = 1.34$$

$$b = 0.537fm, V_0 = -686.4MeV$$

The values of b and V_0 are obtained by reproducing the $N - \Delta$ mass difference and the nucleon mass with a Gaussian single quark orbital wave function, as is used in standard quark model calculations. We also assume a single quark-meson coupling constant, $\frac{g_s^2}{4\pi}$, for all octet mesons (π, K, η) as the originators of the model have done in their calculations. The strange quark mass, m_s , is determined by an overall fit to the masses of the strange baryons. Since "irrespective of the parametrization, the flavor-spin symmetry is essential in the model" [23], we presume that we have maintained the essence of the GBE. In addition,

only the spin-spin component of the pseudoscalar exchange interaction has been included in the calculation. We note that there are extensions of the GBE which include pseudoscalar, vector and scalar meson exchanges with all possible force components [24]. This is expected to be necessary for baryon-baryon interactions, but this addition will be left for future studies.

B. Quark-meson-gluon effective degrees of freedom: FN model

The naive quark-gluon exchange model is quite successful in baryon spectroscopy, but its extension to baryon-baryon interactions is much less so. Only a repulsive core is obtained, but no intermediate range attraction develops in the best studied NN channel. Meson exchange interactions are introduced into the model to provide this well established attraction and the resulting hybrid model with quark, meson and gluon effective degrees of freedom is widely used in baryon interaction calculations. There are several different model variations in this approach. We choose Fujiwara's model (FN) [25] as an example since it gives a simultaneous description of both NN and NY (nucleon-hyperon) interactions.

$$\begin{aligned}
H &= \sum_{i=1}^6 (m_i + \frac{P_i^2}{2m_i}) + \sum_{i<j}^6 (U_{ij}^{Cf} + U_{ij}^{FB} + \sum_{\beta} U_{ij}^{S\beta} + \sum_{\beta} U_{ij}^{PS\beta}) \\
U_{ij}^{Cf} &= -a_c \lambda_i^C \cdot \lambda_j^C r_{ij}^2 \\
U_{ij}^{FB} &= \frac{\alpha_s}{4} \lambda_i^C \cdot \lambda_j^C \left\{ \frac{1}{r_{ij}} - \frac{\pi}{2} \left(\frac{1}{m_i^2} + \frac{1}{m_j^2} + \frac{4}{3} \frac{\sigma_i \cdot \sigma_j}{m_i m_j} \right) \delta(r_{ij}^{\vec{r}}) - \frac{1}{2m_i m_j} \left(\frac{\vec{P}_i \cdot \vec{P}_j}{r_{ij}} + \frac{r_{ij}^{\vec{r}} \cdot (\vec{r}_{ij}^{\vec{r}} \cdot \vec{P}_i) \vec{P}_j}{r_{ij}^3} \right) \right\} \\
U_{ij}^{PS\beta} &= w_{ij}^{PS\beta} \left(\frac{m_{\beta}}{m_{\pi^+}} \right)^2 \frac{m_{\beta}}{3} \left\{ \sigma_i \cdot \sigma_j [Y(x) - c_{\delta} \frac{4\pi}{m_{\beta}^3} \delta(r_{ij}^{\vec{r}})] \right\} \\
U_{ij}^{S\beta} &= -w_{ij}^{S\beta} m_{\beta} Y(x) \\
Y(x) &= \frac{e^{-x}}{x}, \quad x = m_{\beta} |r_{ij}| \\
w_{ij}^{\pi} &= \left(\frac{3}{5} f_8^{PS} \right)^2 \sum_{F=1}^3 \lambda_i^F \lambda_j^F, \quad w_{ij}^K = \left(\frac{3}{5} f_8^{PS} \right)^2 \sum_{F=4}^7 \lambda_i^F \lambda_j^F \\
w_{ij}^{\eta} &= \left(-f_1^{PS} \sin\theta_{PS} + \frac{3}{5} f_8^{PS} \cos\theta_{PS} \lambda_i^8 \right) \times \left(-f_1^{PS} \sin\theta_{PS} + \frac{3}{5} f_8^{PS} \cos\theta_{PS} \lambda_j^8 \right), \\
w_{ij}^{\eta'} &= \left(f_1^{PS} \cos\theta_{PS} + \frac{3}{5} f_8^{PS} \sin\theta_{PS} \lambda_i^8 \right) \times \left(f_1^{PS} \cos\theta_{PS} + \frac{3}{5} f_8^{PS} \sin\theta_{PS} \lambda_j^8 \right) \\
w_{ij}^{\delta} &= (f_8^S)^2 \sum_{F=1}^3 \lambda_i^F \lambda_j^F, \quad w_{ij}^{\kappa} = (f_8^S)^2 \sum_{F=4}^7 \lambda_i^F \lambda_j^F,
\end{aligned}$$

$$w_{ij}^\epsilon = \left(\frac{1}{3}f_1^S \cos\theta_S + f_8^S \sin\theta_S \lambda_i^8\right) \times \left(\frac{1}{3}f_1^S \cos\theta_S + f_8^S \sin\theta_S \lambda_j^8\right),$$

$$w_{ij}^{S*} = \left(-\frac{1}{3}f_1^S \sin\theta_S + f_8^S \cos\theta_S \lambda_i^8\right) \times \left(-\frac{1}{3}f_1^S \sin\theta_S + f_8^S \cos\theta_S \lambda_j^8\right)$$

$$m_{\pi^+} = 140\text{MeV}, m_{\pi^-} = 138\text{MeV}, m_K = 496\text{MeV}, m_\eta = 547\text{MeV}, m_{\eta'} = 958\text{MeV},$$

$$m_\delta = 970\text{MeV}, m_\kappa = 1145\text{MeV}, m_\epsilon = 800\text{MeV}, m_{S^*} = 1250\text{MeV}, c_\delta = 0.381$$

$$f_1^S = 2.89138, f_8^S = 1.07509, f_1^{PS} = 0.21426, f_8^{PS} = 0.26994, \theta_{PS} = -23^\circ, \theta_S = 27.78^\circ$$

$$b = 0.616\text{fm}, a_c = 95.61\text{MeV}\cdot\text{fm}, m_{ud} = 360\text{MeV}, \alpha_s = 2.1742, \lambda = m_s/m_{ud} = 1.526$$

C. Quark-gluon effective degrees of freedom: QDCSM

For this case, we take the quark delocalization, color screening model (QDCSM) as the example [15]. As noted above, the naive quark model with quark and gluon effective degrees of freedom gives a good description of individual baryon properties. However, its extension to baryon-baryon interactions is not successful. The QDCSM maintains quarks and gluons as the effective degrees of freedom, but enlarges the Hilbert space by incorporating quark delocalization. It also distinguishes the confinement potential between quark pairs inside one baryon and from different baryons by introducing color screening. This is based on the recognition that the interaction between quarks from different color singlet baryons must be screened as color neutrality is observed to be maintained on a fm scale. To be precise, the backflow of color necessary is not explicitly modelled, but is accomplished by an effective matrix elements method. The QDCSM gives a reasonable fit to NN, NA and N Σ scattering data.

$$H(6) = \sum_{i=1}^6 \left(m_i + \frac{p_i^2}{2m_i}\right) + \sum_{i<j=1}^6 V_{ij} - T_{CM}$$

$$V_{ij} = V_{ij}^c + V_{ij}^{oge}$$

$$V_{ij}^{oge} = \alpha_s \frac{1}{4} \lambda_i^c \cdot \lambda_j^c \left[\frac{1}{r} - \frac{\pi}{2} \delta(r_{ij}) \left(\frac{1}{m_i^2} + \frac{1}{m_j^2} + \frac{4\sigma_i \sigma_j}{3m_i m_j} \right) + \dots \right]$$

$$V_{ij}^c = \begin{cases} -\lambda_i^c \lambda_j^c a_c r_{ij}^2 & \text{if } i, j \text{ occur in the same baryon orbit} \\ -\lambda_i^c \lambda_j^c \frac{a_c}{\mu} (1 - e^{-\mu r_{ij}^2}) & \text{if } i, j \text{ occur in different baryon orbits} \end{cases}$$

and the delocalized quark orbits are

$$\begin{aligned} \Psi_L(r) &= \frac{(\Phi_L(r) + \epsilon(R_s)\Phi_R(r))}{N(R_s)} \\ \Psi_R(r) &= \frac{(\Phi_R(r) + \epsilon(R_s)\Phi_L(r))}{N(R_s)} \\ N^2(R_s) &= 1 + \epsilon^2(R_s) + 2\epsilon(R_s)\langle\Phi_L|\Phi_R\rangle \end{aligned}$$

where $\phi_L(\phi_R)$ is the left- (right-) centered quark orbital wave function; the mixing parameter $\epsilon(R_s)$ is determined variationally for every R_s by the dynamics of the six-quark system.

$$m_u = m_d = 313\text{MeV}, m_s = 634\text{MeV},$$

$$b = 0.603\text{fm}, \alpha_s = 1.54, a_c = 25.13\text{MeV fm}^{-2}, \mu = 1.0\text{fm}^{-2}.$$

Among these three models, the QDCSM has the fewest parameters.

In order to do a systematic calculation for all three-flavor (u, d, s) six-quark systems, the adiabatic approximation is used to obtain the effective potential between two baryons as a function of their separation. The mass of the six-quark system is then estimated as the sum of the two separate baryon masses, plus the value of the effective potential at its minimum and the zero-point oscillation energy. In the calculation of the six-body matrix elements, the fractional parentage expansion is used. The details of this method can be found in Refs. [15,26]. Such an adiabatic calculation is reasonable for a systematic survey, but only gives a rough estimation of the mass of the six-quark system. A dynamical calculation is needed to obtain quantitative results, but is not expected to lead to significant differences at the level of accuracy of interest here.

III. RESULTS AND DISCUSSION

The baryon-baryon scattering properties calculated are listed in Tables I to VII. Figures 1-12 show the baryon-baryon effective potentials (in units of MeV) as a function of separation

$R(\text{fm})$.

A. Two smearing versions of the GBE model

In a series of papers, Glozman et al. used two different versions of smearing of Goldstone boson exchanges to calculate baryon masses and the NN interaction. We have extended their studies to all possible baryon-baryon S-wave channels consisting of baryon octet and decuplet states and find:

(1) The short-range repulsion obtained from Gaussian smearing is much larger than from Yukawa smearing for some states. Taking the (001) deuteron channel as an example, we find the short-range repulsion is 2436 MeV for Gaussian smearing [22], but only about 790MeV for Yukawa smearing.

(2) Channel coupling has obvious effects for model(a), but negligible effect for model(b). Because of this, some states (about 1/6 of the total) have the similar effective interactions in models (a) and (b) for single channel results, but quite different effective interactions for results from channel coupling. Such states include (-1,3/2,1) (-1,3/2,2) (-201) (-200) (-213) (-221) (-3,1/2,2) (-3,3/2,3) (-402) (-412) , typical examples of which are shown in Fig. 1.

(3) We identify three groups of states, depending on the minimum value of the potential, $|V_0|$:

For the first group, the difference of $|V_0|$ between models (a) and (b) is about 10 MeV. These states include most of the states with small angular momentum ($J = 0, 1$). These states, including (021), (030), (-1,1/2,2), (-1,3/2,0), (-1,5/2,0), (-2,0,2), (-2,2,0), (-5,1/2,0), (-6,0,2) and so on, are not sensitive to the different forms of smearing of the δ -function, typical examples of which are shown in Fig. 2.

For the second group, the difference of $|V_0|$ values between model(a) and (b) is greater than 20 MeV, but not more than 100 MeV. For these states, intermediate-range attraction is always present, but the strength of the attraction varies with the form of smearing. Many states with large angular momentum ($J = 3$) belong to this group, such as (003), (013),

(-203), (-3,1/2,0), (-3,1/2,3), (-403) and so on. (See Fig. 2). As for the first group, the results do not depend sensitively on the form of the choice of smearing.

The difference between models (a) and (b) shows up most strongly for the third group of states. Comparing the results for (023), (022), (033), (-1,3/2,3), (-1,5/2,3), (-1,5/2,2), (-213), (-3,3/2,0), (-3,3/2,3), (-5,1/2,2), (-5,1/2,3), and (-603), (see Fig. 3,) we find a very small value for $|V_0|$, or even no attraction at all, in model (b), while we find a very large value for $|V_0|$, in the range of 200 to 400 MeV at small equilibrium separation ($R_s = 0.5 - 0.8 fm$) in model (a).

In the following comparisons, when we refer to the GBE model, we will mean model (b), because it is consistent with the requirement that the volume integral of the pseudoscalar meson exchange interaction should vanish.

B. Comparison among the three different models

All possible S-wave states of (SIJ) obtained from the ground state octet and decuplet baryons in the u, d, and s three-flavor world have been calculated with the three models (GBE(a) and (b), FN and QDCSM) based on three sets of effective degrees of freedom. We will discuss the general features first and then the details for some interesting aspects.

1. General features

(1) Deuteron properties: Since the deuteron is a well known, stable, two-nucleon state ($SIJ = 001$), we take it as a measure of the precision of our model calculation. The three different models all show a weak attraction; the minimum of the effective potential is -18 MeV (FN), -21 MeV (QDCSM), -3 MeV (GBE), and the separation corresponding to the minimum energies is 1.2fm, 1.3fm, 2.0fm, respectively. These reproduce the deuteron channel NN interaction qualitatively, but the estimated masses in the three models differ by 15-27 MeV from the deuteron energy. The main causes of this deviation are twofold: First, the S-D wave mixing due to the one pion exchange tensor interaction has not been

taken into account; second the adiabatic approximation and zero-point harmonic oscillation energy used in this calculation are rough approximations. A dynamical calculation with the extended QDCSM, where the one pion exchange tensor interaction is included, does reproduce the deuteron energy, size and D-wave mixing accurately [15]. This emphasizes that the results reported here only produce a qualitative effective baryon-baryon interaction. To study dibaryon states, a careful dynamical calculation is needed. In fact, if the deuteron would not have been found by experiment, it would have been difficult for any of the models to predict its existence.

(2) Quark delocalization effect: For Fujiwara's quark-meson-gluon coupling model, enlarging the model space will not change the results, i.e., systems always prefer to remain with small delocalization ($\epsilon \leq 0.1$)¹, even for those states with minimum energy at small separations. A similar conclusion follows for both of Glozman's quark-meson coupling models, (a) and (b). On the other hand, for the QDCSM, the quark delocalization effect is obvious. For some states the delocalization parameter ϵ can reach 1.0 at the minimum energy of the system. Quark delocalization compensates for the explicit meson exchange effect absent in the QDCSM.

(3) Channel coupling effect: In all of these three models, the channel coupling effect is small for most cases; the largest effect is about 50-100MeV. For those channels where the binding energy is close to the channel threshold, channel coupling may well play a critical role in forming dibaryon states. Jaffe's H particle case is a clear example. In those cases, the channel coupling should be studied dynamically.

2. Details

From the calculated results of three different models, we found that about two-thirds of the states within the u, d, and s three-flavor world have quite similar, and in some cases

¹In Tables III–VII, ϵ is omitted for the FN model.

indistinguishable, effective baryon-baryon interactions:

(1) States with the same, purely repulsive, interaction:

States with almost the same effective repulsive baryon-baryon interactions include (000), (011), (023), (022), (033), (032), (-1,3/2,2), (-1,3/2,1), (-1,5/2,3), (-1,5/2,2), (-221), (-403), (-411), (-5,1/2,3), (-5,1/2,2), (-603) and (-602). These states have purely repulsive potentials in all three models despite their different effective degrees of freedom. There are altogether 17 states, among all 64 states of 6-quark system, belonging to this case. To simplify the presentation, only the four states which have different strangeness are shown in Fig.4.

(2) States with similar weak attraction :

(i) Some states have very similar baryon-baryon interactions for all three models, all producing a weak attraction, with the minimum energies of the systems appearing at large separation. (The separation is a bit smaller for a few states in the FN model). We find 13 states belonging to this case, such as (001), (010), (021), (-1,1/2,1), (-1,3/2,0), (-201), (-211), (-210), (-222), (-3,3/2,2), (-3,3/2,1), (-402) and (-400). Typical ones are shown in Fig.5. Because the binding energies of these states are small, their masses are close to the corresponding thresholds. Whether the binding energy is positive or negative is very sensitive to the details of the models. It is difficult to determine whether these are strong interaction stable states or not, since the precision of the adiabatic approximation is limited. A dynamical calculation is especially needed in these cases in order to obtain more reliable results.

(ii) There are states for which the QDCSM and FN give quite similar results, but the GBE model yields an even weaker attraction. States belonging to this case include (031), (-3,1/2,1), (-401) and (-412), two of which are shown in Fig.6. The QDCSM and FN model obtain a minimum of the effective attraction of several tens of MeV, or at most a hundred MeV, but the GBE model yields only several MeV for these states.

(iii) There are states for which the QDCSM and GBE models obtain a weak attraction, while the FN model yields a little stronger attraction. These states include: (-1,1/2,0), (-1,5/2,1), (-220) and (-3,1/2,0), as shown in Fig.7. For these states, the QDCSM and GBE

models obtain a minimum of several MeV, while in the FN model, the minimum is several tens of MeV.

(iv) For some states, the QDCSM obtains a somewhat stronger attraction than either of the other two models. Such states include: (012), (-223) and (-413); the latter two are shown in Fig.8.

(v) Finally, there are states for which the FN and GBE models obtain slightly different effective potentials with the results of the QDCSM in between. For the states (020), (030) and (-1,5/2,0), the latter two of which are shown in Fig.9, the GBE model yields a strong repulsive core and weak intermediate-range attraction; the FN model obtains a weak repulsive core and considerable intermediate-range attraction, and the QDCSM obtains, on the one hand, a repulsive core similar to that of the GBE model, and on the other, an intermediate-range attraction similar to that of the FN model.

Altogether, we find that the three different models based on the three different effective degrees of freedom not only all give a good description of baryon spectra, but they also give similar effective baryon-baryon interactions for two thirds of all of the states possible within the three-flavor world. This implies that, with regard to baryon spectra and baryon-baryon interactions, the models based on the different effective degree of freedoms are still compatible. We infer that quark delocalization and color screening, working together in the QDCSM, must provide a good representation of meson exchange effects at some level of accuracy. All of this appears consistent with old conclusions developed from nonperturbative QCD: Models with different effective degrees of freedom but with physically equivalent results can be obtained for low energy QCD under different approximations.

Each model has distinct characteristics with respect to the remaining one third of the states:

(1) The QDCSM predicts strong intermediate-range attraction for states with large angular momentum. As the strangeness becomes more negative, the minimum of the effective potential, V_0 , becomes less negative, as can be seen from the sequence: (003) with $V_0 = -359\text{MeV}$, (-1,1/2,3) with $V_0 = -308\text{MeV}$, (-202) with $V_0 = -184\text{MeV}$, and (-403)

where $|V_0|$ is only several MeV. (See Fig.10.)

(2) The FN model predicts a weak attraction in the effective potential for states with small strangeness. Conversely to the QDCSM, here, as the strangeness becomes more negative, $|V_0|$ also becomes more negative. For example, for the state $(-3,3/2,0)$ $V_0 = -87\text{MeV}$, for (-410) $V_0 = -95\text{MeV}$, for $(-5,1/2,1)$ $V_0 = -136\text{MeV}$, and for (-600) $V_0 = -281\text{MeV}$. (See Fig.11.)

The Darwin term of the Breit-Fermi interaction has been included in the FN model. We find its contribution to the baryon-baryon effective interaction to be small, typically giving rise to a weak attraction with a minimum $\leq 10\text{MeV}$.

(3) Since the GBE model that we used in our calculations does not take into account scalar and vector meson contributions, the effective interaction obtained is usually less attractive than the other two models. One would expect that the GBE will give more similar results if these exchanges are incorporated.

3. Particularly interesting states

(1) d^* dibaryon state (003); (see Fig.10): The QDCSM predicts this to be a tightly bound, 6-quark state, but the other models predict only a weak intermediate-range attraction, which does not provide enough attraction to form a bound state relative to $NN\pi\pi$ threshold. Recently, a dynamical calculation in the QDCSM obtained a slightly smaller binding energy for the d^* ($\sim 2.18\text{GeV}$) [15]. The difference is due to the fact that the zero-point oscillation energy in this case underestimates the relative kinetic energy of the two baryons. However the d^* mass is still much lower than found in the other models.

(2) Di- Ω state (-600); (see Fig.11): The FN model predicts a strong intermediate-range attraction with binding energy $B = -62\text{MeV}$. The mass of the state is 3282 MeV , which is lower than the $\Omega\Omega$ threshold 3345MeV , so that a strong interaction stable state is predicted. Another hybrid model [27] obtains a similar result; (B is about -100 MeV). The GBE model predicts $B = -11\text{ MeV}$. This mass is slightly lower than the threshold, and is expected

to decrease further if scalar and vector meson exchanges are incorporated. The QDCSM predicts a mass of 3350 MeV, but a dynamical calculation obtains a smaller mass, which is closer to the results of the hybrid models. In this case, the zero-point harmonic oscillation energy overestimates the relative kinetic energy.

(3) H particle (-200); (see Fig.12): The QDCSM predicts that this is a strong interaction stable state with small binding energy, $B = -14$ MeV; the mass is 2218 MeV. The FN model obtains a mass of 2312 MeV, which is higher than the threshold (2231MeV). Zhang's dynamical calculation obtains a mass for the H close to the $\Lambda\Lambda$ threshold [28]. The GBE(a) model obtains 2207 MeV, which is a little lower than the threshold, while GBE(b) obtains 2249 MeV, which is a little higher than the threshold. Almost all of these model results are close to the $\Lambda\Lambda$ threshold. Taken together, they imply that the mass of the H particle is sensitive to model details. Experimental searches should (and do) take into account the two possibilities of a strong interaction stable state with long lifetime, as well as a narrow resonances with a short lifetime.

IV. CONCLUSION

The three constituent quark models based on quark-meson, quark-gluon and quark-meson-gluon effective degrees of freedom are widely used in the study of hadron spectroscopy and hadron interaction, and there is a hot debate about which degrees of freedom are the proper ones [21]. For the 64 two baryon channels consisting of octet and decuplet baryons, we find that the three models give similar effective baryon-baryon interactions for about 2/3 of these channels. The three models appear to be different, but in fact are not very different in describing effective baryon-baryon interactions.

For some time, a number of authors have viewed the QDCSM as an exceptional model. Some have even claimed that it violates principles of quantum mechanics [29]. This is incorrect, as it is a conventional effective matrix element approach, which we have proposed because of our concern regarding a sound theoretical basis for direct extension of the two

body confinement interaction from single to multi-hadron systems, where nonlinearity may be expected to be significant. Quark model studies of multi-hadron systems provide important checks of the model descriptions of confinement. The results of this paper demonstrate that predictions of the QDCSM are not so exceptional as might appear from its definition. On the contrary, it embodies meson exchange effects in its own way, i.e., through quark delocalization and a different parametrization of quark confinement. Since the effective matrix element method is widely used in the Heisenberg version of matrix mechanics, we are at a loss to explain how the authors of Ref. [29] have so misunderstood our model as to arrive at such incorrect conclusions regarding it.

This paper also demonstrates that there are differences among these three models. This has been shown in baryon spectroscopy [21]. It also appears in the predictions for different dibaryon masses, especially for states of high spin and high strangeness. More precise hadron spectroscopy and experimental study of the dibaryon states predicted by these models are needed to distinguish which degree of freedom best describes low energy hadron physics.

This research is partly supported by the NSF, SED and SSTD of China, and partly by the US Department of Energy under contract W-7405-ENG-36.

REFERENCES

- [1] D.Richards, nucl-th/0011012.
- [2] H.Yukawa, Proc.Phys.Math.Soc.Jpn. **17**, 48 (1935).
- [3] R.Machleidt, Nucl.Phys.**A** (nucl-th/0009055).
- [4] S.Weinberg, Physica**96A**, 327 (1979); Phys.Lett. **B251**, 288 (1990); Nucl.Phys.**B363**, 3 (1991); Phys.Lett.**B295**, 114 (1992).
- [5] Q.Wang, Y.P.Kuang, X.L.Wang and M.Xiao, Phys.Rev. **D61**, 54011 (2000).
- [6] R.T.Cahill and C.D.Roberts, Phys.Rev.**D32**, 2419 (1985).
- [7] P.C.Tandy, Prog.Part.Nucl.Phys.**39**, 117 (1997).
R.T.Cahill and S.M.Gunner, Fizika**B7**, 17 (1998).
X.F.Lu, Y.X.Liu, H.S.Zong, E.G.Zhao, Phys.Rev.**C58**, 1195 (1998).
- [8] L.Ya.Glozman and D.O.Riska, Phys.Rep.**268**, 263 (1996).
D.O.Riska and G.E.Brown, Nucl.Phys.**A653**, 251 (1999).
- [9] A.Manohar and H.Georgi, Nucl.Phys.**B234**, 189 (1984).
- [10] S.Takeuchi, K.Shimizu and K.Yazaki, Nucl.Phys. **A504**, 777 (1989).
A.Valcarcer, A.Buchmann, F.Fernandez, A.Faessler, Phys.Rev. **C50**, 2246 (1994); **C51**, 1480 (1995).
Y.Fujiwara, C.Nakamoto and Y.Suzuki, Phys.Rev.Lett.**76**, 2242 (1996).
- [11] A.De Rujula, H.Georgi and S.L.Glashow, Phys.Rev.**D12**, 147 (1975).
N.Isgur and G.Karl, Phys.Rev.**D18**, 4187 (1978); **D19**, 2653 (1979); **D20**, 1191 (1979).
- [12] E.Gubankova, C.R.Ji and S.R.Cotanch, hep-ph/9908331.
- [13] C.D.Roberts and S.M.Schmidt, Prog.Part.Nucl.Phys.**45S1**, 1-103, (2000).
- [14] M.Oka and K.Yazaki, "Quarks in Nuclei", International Review of Nuclear Physics,

- Vol.1, ed. W.Weise (World Scientific, Singapore, 1985), p.489.
- C.W.Wong, Phys.Rep.**136**, 1 (1986).
- F.Myhrer and J.Wroldsm, Rev.Mod.Phys.**60**, 629 (1988).
- K.Shimizu, Rep.Prog.Phys.**52**, 1 (1989).
- [15] F.Wang et al., Phys.Rev.Lett.**69**, 2901 (1992).
 G.H.Wu et al., Phys.Rev.**C53**, 1161 (1996); Nucl.Phys.**A673**, 279 (2000).
 J.L.Ping, F.Wang and T.Goldman, nucl-th/0012011.
- [16] A.Chodos, R.L.Jaffe, K.Johnson, C.B.Thorn and V.Weisskopf, Phys.Rev.**D9**, 3471 (1974).
- [17] A.Chodos and C.B.Thorn, Phys.Rev.**D12**, 2733 (1975).
 A.W.Thomas, J.Phys.**G7**, L283, (1981).
 G.E.Brown and M.Rho, Phys.Lett.**B82**, 177 (1979).
- [18] R.L.Jaffe and F.E.Low, Phys.Rev.**D19**, 2105 (1979).
 P.LaFrance and E.L.Lomon, Phys.Rev.**D34**, 1341 (1986) and references therein.
 A.M.Badalyan and Yu.A.Simonov, Yad.Fiz.**36**, 1479 (1982).
 Yu.A.Simonov, Nucl.Phys.**A416**, 109c (1984); **A463**, 231c (1987).
- [19] I.Zahed and G.E.Brown, Phys Reports, **142**, 1 (1986).
- [20] R.Friedberg and T.D.Lee, Phys.Rev.**D15**, 1694 (1977); **D16**, 1096 (1977).
 M.R.Frank and P.C.Tandy, Phys.Rev.**C46**, 338 (1992).
- [21] N.Isgur, Phys.Rev.**D61**, 118501; **D62**, 054026 (2000).
 L.Ya.Glozman, nucl-th/9909021.
 H.Collins and H.Georgi, Phys.Rev.**D59**, 094010 (1999).
 K.F.Lin et.al., Phy.Rev.**D59**, 112001 (1999); **D61**, 118502 (2000).
- [22] L.Ya.Glozman, Z.Papp, W.Plessas, Phys.Lett.**B381**, 311 (1996).
 Fl.Stancu, S.Pepin and L.Ya.Glozman, Phys.Rev.**C56**, 2779 (1997).

- L.Ya.Glozman, Z.Papp, W.Plessas et al. Nucl.Phys.**A623**, 90c (1997).
- M.Genovese, J.M.Richard, Fl.Stancu and S.Pepin, Phys.Lett. **B625**, 171 (1998).
- D.Bartz and Fl.Stancu, Phys. Rev.**C59**, 1756 (1999); **C60**, 055207 (1999).
- [23] L.Ya.Glozman, W.Plessas, K.Varga and R.F.Wagenbrunn, Phys.Rev.**D58**, 094030 (1998).
- D.Bartz and Fl.Stancu, Phys.Rev.**C63**, 034001 (2001).
- [24] L.Ya.Glozman, Nucl.Phys.**A663-664**, 103c (2000).
- R.F.Wagenbrunn, L.Ya.Glozman, W.Plessas, K.Varga, Nucl.Phys. **A663-664**, 703c (2000).
- [25] Y.Fujiwara, C.Nakamoto and Y.Suzuki, Phys.Rev.**C54**, 2180 (1996).
- [26] F.Wang et al., Phys.Rev.**C51**, 3411 (1995).
- J.L.Ping, et al., Nucl.Phys.**A657**, 95 (1999).
- [27] Q.B.Li, P.N.Shen, Z.Y.Zhang and Y.W.Yu, Nucl.Phys.**A683**: 487-509 (2001).
- [28] P.N.Shen, Z.Y.Zhang, et al., J.Phys.**G25**, 1807 (1999).
- P.N.Shen, Z.Y.Zhang, et al., Chin.Phys.Lett. (1999) (in press).
- [29] X.Q.Yuan, Z.Y.Zhang, Y.W.Yu and P.N.Shen, Phys.Rev. **C60**, 045203 (1999).

Table I: An asymptotic two-baryon system with channel quantum numbers and delocalization parameter values (ϵ) in GBE(a) and (b) for $S = 0, -1, -2$. The notation is as follows: sc stands for single channel; cc stands for multichannel coupling; B_α is the binding energy; E_α is the mass and V_0 is the potential energy at the equilibrium separation, R_s ; (SIJ) are the strangeness, isospin and total angular momentum quantum numbers for each channel.

Table I		GBE(a)					GBE(b)					Threshold
SIJ		E_α	V_0	B_α	ϵ	R_s	E_α	V_0	B_α	ϵ	R_s	
0, 0, 1	sc	1889	-1	11	0.0	2.3	1891	-3	13	0.0	2.0	1878(NN)
	cc	1889	-1	11	0.0	2.3	1891	-3	13	0.0	2.0	
0, 0, 3	sc	2503	-35	39	0.1	0.7	2474	-14	10	0.1	1.4	2464($\Delta\Delta$),2158($NN\pi\pi$)
0, 1, 0	sc	1888	-1	10	0.0	2.4	1892	-3	14	0.0	1.9	1878(NN)
	cc	1888	-1	10	0.0	2.4	1892	-3	14	0.0	1.9	
0, 2, 3	sc	2333	-205	-131	0.0	0.8	2471	-1	7	0.0	2.6	2464($\Delta\Delta$),2158($NN\pi\pi$)
-1, 1/2, 3	sc	2621	-40	5	0.1	1.0	2619	-24	2	0.1	1.3	2617($\Delta\Sigma^*$)
	cc	2638	-49	21	0.1	0.8	2619	-24	2	0.1	1.3	2335($N\Lambda\pi\pi$)
-1, 3/2, 0	sc	2141	-1	9	0.0	2.4	2144	-3	12	0.0	1.9	2132($N\Sigma$)
	cc	2141	-1	9	0.0	2.4	2144	-3	12	0.0	1.9	
-1, 3/2, 3	sc	2523	-164	-94	0.0	0.8	2623	-1	6	0.0	2.5	2617($\Delta\Sigma^*$)
	cc	2523	-164	-94	0.0	0.8	2629	-10	13	0.1	1.4	2335($N\Lambda\pi\pi$)
-2, 0, 0	sc	2239	0	8	0.0	-	2245	0	14	0.0	-	2231($\Lambda\Lambda$)
	cc	2207	-106	-24	0.0	0.8	2249	-1	18	0.0	1.7	
-2, 0, 2	sc	2481	-1	9	0.0	2.3	2487	-3	15	0.0	1.7	2472($N\Xi^*$)
	cc	2481	-1	9	0.0	2.3	2487	-3	15	0.0	1.7	2397($N\Xi\pi$)
-2, 0, 3	sc	2785	-26	16	0.1	1.0	2779	-3	10	0.0	1.8	2770($\Sigma^*\Sigma^*$)
-2, 1, 3	sc	2762	-56	-3	0.1	0.9	2775	-16	10	0.1	1.3	2765($\Delta\Xi^*$)
	cc	2701	-117	-64	0.0	0.9	2765	-36	-1	0.1	1.1	2690($\Delta\Xi\pi$)
-2, 2, 0	sc	2393	-1	7	0.0	2.5	2397	-3	11	0.0	1.9	2386($\Sigma\Sigma$)
	cc	2393	-1	7	0.0	2.5	2400	-3	14	0.0	1.7	
-2, 2, 2	sc	2559	0	9	0.0	-	2560	-1	10	0.0	2.1	2550($\Xi\Delta$)
	cc	2262	-471	-288	0.0	0.5	2568	-9	18	0.1	1.3	
-2, 2, 3	sc	2635	-197	-131	0.0	0.8	2766	0	1	0.0	-	2765($\Delta\Xi^*$)
	cc	2491	-393	-274	0.0	0.6	2769	-22	3	0.1	1.3	2690($\Delta\Xi\pi$)

Table II: The same as Table I for states with $S = -3, -4, -5, -6$.

Table II		GBE(a)					GBE(b)					Threshold
SIJ		E_α	V_0	B_α	ϵ	R_s	E_α	V_0	B_α	ϵ	R_s	
-3, 1/2, 0	sc	2440	0	7	0.0	-	2449	-1	15	0.0	1.7	2434($\Lambda\Xi$)
	cc	2444	-50	10	0.0	0.9	2455	-3	22	0.0	1.4	
-3, 1/2, 3	sc	2867	-100	-51	0.0	0.9	2924	-1	6	0.0	2.4	2918($\Xi^*\Sigma^*$)
	cc	2867	-100	-51	0.0	0.9	2930	-9	12	0.1	1.4	
-3, 3/2, 0	sc	2361	-197	-150	0.0	1.0	2523	-7	21	0.1	1.3	2511($\Sigma\Xi$)
	cc	2290	-513	-221	0.0	0.4	2534	-10	23	0.1	1.2	
-3, 3/2, 3	sc	2874	-81	-30	0.1	0.9	2917	-11	13	0.1	1.3	2904($\Delta\Omega$) 2714($\Lambda\Xi\pi\pi$)
	cc	2701	-318	-203	0.0	0.6	2892	-54	-12	0.1	1.0	
-4, 0, 0	sc	2637	0	1	0.0	-	2654	-5	18	0.0	1.4	2636($\Xi\Xi$)
	cc	2637	0	1	0.0	-	2654	-5	18	0.0	1.4	
-4, 0, 3	sc	3038	-76	-29	0.0	0.9	3073	-1	6	0.0	2.4	3066($\Xi^*\Xi^*$)
-4, 1, 2	sc	2828	-52	-23	0.0	1.2	2852	0	1	0.0	-	2851($\Xi\Xi^*$)
	cc	2657	-360	-195	0.0	0.5	2873	-13	21	0.1	1.1	
-4, 1, 3	sc	2998	-107	-59	0.0	0.9	3063	0	6	0.0	-	3057($\Sigma^*\Omega$)
	cc	2876	-288	-181	0.0	0.6	3068	-12	11	0.1	1.3	
-5, 1/2, 2	sc	2907	-123	-83	0.0	1.0	2991	0	1	0.0	-	2990($\Xi\Omega$)
	cc	2778	-322	-212	0.0	0.6	2998	0	7	0.0	-	
-5, 1/2, 3	sc	3025	-256	-181	0.0	0.7	3207	0	1	0.0	-	3205($\Xi^*\Omega$)
	cc	3025	-256	-181	0.0	0.7	3213	0	7	0.0	-	
-6, 0, 0	sc	3350	0	5	0.0	2.6	3334	-40	-11	0.1	1.1	3345($\Omega\Omega$)
-6, 0, 1	sc	3350	0	5	0.0	2.6	3355	-11	10	0.1	1.3	
-6, 0, 3	sc	3198	-218	-147	0.0	0.7	3346	0	1	0.0	-	

Table III: An asymptotic two-baryon system with channel quantum numbers and delocalization parameter values (ϵ) in the QDCSM, GBE and FN models for $S = 0$. The notation is the same as Table I. (For the FN model, ϵ is omitted.)

Table III		GBE(b)					FN				QDCSM					Threshold
SIJ		E_α	V_0	B_α	ϵ	R_s	E_α	V_0	B_α	R_s	E_α	V_0	B_α	ϵ	R_s	
0, 0, 0	sc	1879	0	1	0.0	-	1879	0	1	-	1879	0	1	0.0	-	1878(NN)
	cc	1888	4	10	0.0	-	1887	2	9	-	1885	0	7	0.0	-	
0, 0, 1	sc	1891	-3	13	0.0	2.0	1903	-18	25	1.2	1885	-20	7	0.1	1.5	
	cc	1891	-3	13	0.0	2.0	1903	-18	25	1.2	1894	-21	16	0.2	1.3	
0, 0, 2	sc	2478	-14	14	0.1	1.3	2479	-24	15	1.1	2259	-233	-205	1.0	1.3	2464($\Delta\Delta$)
0, 0, 3	sc	2474	-14	10	0.1	1.4	2479	-24	15	1.1	2144	-359	-320	1.0	1.1	2158($NN\pi\pi$)
0, 1, 0	sc	1892	-3	14	0.0	1.9	1906	-35	28	1.0	1893	-10	15	0.1	1.6	1878(NN)
	cc	1892	-3	14	0.0	1.9	1905	-35	27	1.0	1892	-9	14	0.1	1.6	
0, 1, 1	sc	1879	0	1	0.0	-	1879	0	1	-	1879	0	1	0.0	-	
	cc	1885	0	7	0.0	-	1890	0	12	0.0	1885	0	7	0.0	-	
0, 1, 2	sc	2182	-2	11	0.0	2.1	2185	-14	14	1.4	2122	-87	-49	0.4	1.2	2171($N\Delta$)
	cc	2181	-4	11	0.0	1.9	2185	-14	14	1.4	2122	-87	-49	0.4	1.2	2018($NN\pi$)
0, 1, 3	sc	2472	-4	8	0.0	2.0	2476	-3	12	1.8	2304	-188	-160	1.0	1.3	2464($\Delta\Delta$)
0, 2, 0	sc	2476	-12	12	0.1	1.4	2442	-80	-22	0.9	2383	-105	-81	0.4	1.4	
0, 2, 1	sc	2181	-5	10	0.0	1.9	2170	-39	1	1.2	2169	-24	-2	0.1	1.6	2171($N\Delta$)
	cc	2181	-5	10	0.0	1.9	2186	-40	15	1.0	2169	-24	-2	0.1	1.6	2018($NN\pi$)
0, 2, 2	sc	2172	0	1	0.0	-	2172	0	1	-	2172	0	1	0.0	-	
	cc	2180	-1	9	0.0	-	2172	0	6	-	2172	0	6	0.0	-	
0, 2, 3	sc	2471	-1	7	0.0	-	2470	0	6	-	2442	-41	-22	0.6	1.6	2464($\Delta\Delta$)
0, 3, 0	sc	2471	-11	7	0.0	1.6	2385	-153	-79	0.8	2416	-69	-48	0.2	1.5	
0, 3, 1	sc	2473	-6	9	0.0	1.8	2440	-63	-24	1.1	2451	-32	-13	0.2	1.6	
0, 3, 2	sc	2472	-1	8	0.0	2.3	2474	-3	10	1.9	2474	-2	10	0.1	2.0	
0, 3, 3	sc	2465	0	1	0.0	-	2465	0	1	-	2465	0	1	0.0	-	

Table IV: The same as Table III for $S = -1$.

Table IV		GBE(b)					FN				QDCSM					Threshold
SIJ		E_α	V_0	B_α	ϵ	R_s	E_α	V_0	B_α	R_s	E_α	V_0	B_α	ϵ	R_s	
-1, 1/2, 0	sc	2056	0	1	0.0	-	2056	0	1	-	2056	0	1	0.0	-	2055($N\Lambda$)
	cc	2070	-2	16	0.0	1.8	2090	-35	35	0.9	2072	-5	17	0.1	1.6	
-1, 1/2, 1	sc	2056	0	1	0.0	-	2065	0	11	2.3	2056	0	1	0.0	-	2324($N\Sigma^*$)
	cc	2071	-1	17	0.0	1.8	2095	-10	38	1.1	2077	-17	23	0.2	1.2	
-1, 1/2, 2	sc	2334	-2	11	0.0	2.0	2339	-12	15	1.4	2255	-111	-68	0.4	1.1	2617($\Delta\Sigma^*$)
	cc	2337	-3	13	0.0	1.8	2359	-16	36	1.0	2227	-161	-96	1.0	0.9	
-1, 1/2, 3	sc	2619	-24	2	0.1	1.3	2630	-4	14	1.6	2346	-308	-271	1.0	1.1	2335($N\Lambda\pi\pi$)
	cc	2619	-24	2	0.1	1.3	2631	-23	14	1.1	2346	-308	-271	1.0	1.1	
-1, 3/2, 0	sc	2144	-3	12	0.0	1.9	2143	-27	11	1.2	2138	-18	6	0.1	1.5	2132($N\Sigma$)
	cc	2144	-3	12	0.0	1.9	2156	-45	24	0.9	2138	-18	6	0.1	1.5	
-1, 3/2, 1	sc	2133	0	1	0.0	-	2133	0	1	-	2133	0	1	0.0	-	2324($N\Sigma^*$)
	cc	2133	0	1	0.0	-	2133	0	1	-	2133	0	1	0.0	-	
-1, 3/2, 2	sc	2325	0	1	0.0	-	2325	0	1	-	2325	0	1	0.0	-	2617($\Delta\Sigma^*$)
	cc	2330	0	6	0.0	-	2331	0	8	-	2333	-17	9	0.2	1.4	
-1, 3/2, 3	sc	2623	-1	6	0.0	-	2622	0	5	-	2512	-131	-105	0.6	1.3	2335($N\Lambda\pi\pi$)
	cc	2629	-10	13	0.1	1.4	2628	-1	11	1.9	2512	-131	-105	0.6	1.3	
-1, 5/2, 0	sc	2621	-19	4	0.1	1.4	2520	-167	-97	0.8	2578	-61	-38	0.2	1.4	2425($\Delta\Sigma$)
	cc	2621	-19	4	0.1	1.4	2520	-167	-97	0.8	2578	-61	-38	0.2	1.4	
-1, 5/2, 1	sc	2435	-2	10	0.0	2.0	2420	-39	-5	1.2	2423	-21	-2	0.1	1.6	2617($\Delta\Sigma^*$)
	cc	2437	-5	12	0.0	1.7	2418	-66	-7	0.9	2424	-25	-1	0.2	1.4	
-1, 5/2, 2	sc	2426	0	1	0.0	-	2426	0	1	-	2426	0	1	0.0	-	2335($N\Lambda\pi\pi$)
	cc	2431	0	6	0.0	-	2430	0	5	-	2430	0	5	0.0	-	
-1, 5/2, 3	sc	2618	0	1	0.0	-	2618	0	1	-	2681	0	2	0.0	-	2617($\Delta\Sigma^*$)
	cc	2618	0	1	0.0	-	2618	0	1	-	2623	-7	6	0.2	1.8	

Table V: The same as Table III for $S = -2$.

Table V		GBE(b)					FN				QDCSM					Threshold
SIJ		E_α	V_0	B_α	ϵ	R_s	E_α	V_0	B_α	R_s	E_α	V_0	B_α	ϵ	R_s	
-2, 0, 0	sc	2245	0	14	0.0	1.9	2302	-36	71	0.7	2249	-5	18	0.1	1.5	2231($\Lambda\Lambda$)
	cc	2249	-1	18	0.0	1.7	2312	-65	81	0.6	2218	-159	-14	1.0	0.6	
-2, 0, 1	sc	2232	0	1	0.0	-	2245	-1	14	1.9	2232	0	1	0.0	-	
	cc	2237	0	6	0.0	-	2329	-9	98	0.7	2300	-38	69	1.0	0.7	
-2, 0, 2	sc	2487	-3	15	0.0	1.7	2488	-10	16	1.4	2476	-173	-102	0.7	0.8	2472($N\Xi^*$)
	cc	2487	-3	15	0.0	1.7	2515	-35	43	0.8	2367	-184	-106	1.0	0.8	2397($N\Xi\pi$)
-2, 0, 3	sc	2779	-3	10	0.0	1.8	2782	-6	13	1.5	2656	-142	-113	0.7	1.2	2770($\Sigma^*\Sigma^*$)
-2, 1, 0	sc	2258	0	1	0.0	-	2258	0	1	-	2258	0	1	0.0	-	2257($N\Xi$)
	cc	2253	0	6	0.0	-	2310	-31	53	0.8	2277	-7	20	0.1	1.4	
-2, 1, 1	sc	2267	0	10	0.0	2.3	2274	-2	16	1.7	2276	-5	19	0.1	1.5	
	cc	2268	0	11	0.0	2.2	2322	-19	65	0.8	2290	-33	33	0.4	0.9	
-2, 1, 2	sc	2473	0	1	0.0	-	2473	0	1	-	2362	-260	-188	1.0	0.8	2472($N\Xi^*$)
	cc	2478	0	6	0.0	-	2480	0	8	-	2422	-129	-50	1.0	0.8	
-2, 1, 3	sc	2775	-16	10	0.1	1.3	2781	-3	16	1.5	2560	-251	-209	1.0	1.0	2765($\Delta\Xi^*$)
	cc	2765	-36	-1	0.1	1.1	2782	-18	17	1.1	2557	-251	-209	1.0	1.0	2690($\Delta\Xi\pi$)
-2, 2, 0	sc	2397	-3	11	0.0	1.9	2405	-57	19	0.8	2397	-11	11	0.1	1.5	2386($\Sigma\Sigma$)
	cc	2400	-3	14	0.0	1.7	2400	-62	14	0.8	2397	-11	11	0.1	1.5	
-2, 2, 1	sc	2387	0	1	0.0	-	2387	0	1	-	2387	0	1	0.0	-	
	cc	2387	0	1	0.0	-	2387	0	1	-	2387	0	1	0.0	-	
-2, 2, 2	sc	2560	-1	10	0.0	2.1	2561	-2	11	1.9	2531	-57	-19	0.5	1.1	2550($\Delta\Xi$)
	cc	2568	-9	18	0.1	1.3	2588	-19	38	0.9	2530	-52	-20	0.3	1.2	
-2, 2, 3	sc	2766	0	1	0.0	-	2766	0	1	-	2713	-82	-52	0.6	1.2	2765($\Delta\Xi^*$)
	cc	2769	-22	3	0.1	1.3	2766	0	1	-	2717	-74	-49	0.4	1.3	2690($\Delta\Xi\pi$)

Table VI: The same as Table III for $S = -3, -6$.

Table VI		GBE(b)					FN				QDCSM					Threshold
SIJ		E_α	V_0	B_α	ϵ	R_s	E_α	V_0	B_α	R_s	E_α	V_0	B_α	ϵ	R_s	
-3, 1/2, 0	sc	2449	-1	15	0.0	1.7	2453	-21	19	1.1	2444	-19	10	0.1	1.3	2434($\Xi\Lambda$)
	cc	2455	-3	22	0.0	1.4	2469	-63	36	0.7	2443	-19	9	0.1	1.3	
-3, 1/2, 1	sc	2435	0	1	0.0	-	2444	0	10	-	2528	-99	94	1.0	0.5	2611($N\Omega$)
	cc	2495	-37	61	0.1	0.7	2485	-83	51	0.6	2520	-107	86	1.0	0.5	
-3, 1/2, 2	sc	2623	0	12	0.0	2.0	2629	-1	18	1.6	2552	-271	-151	1.0	0.6	2574($\Lambda\Xi\pi$)
	cc	2656	-15	45	0.1	0.9	2672	-38	61	0.7	2548	-198	-64	1.0	0.6	
-3, 1/2, 3	sc	2924	-1	6	0.0	2.4	2923	0	5	-	2836	-115	-82	0.6	1.1	2918($\Sigma^*\Xi^*$)
	cc	2930	-9	12	0.1	1.4	2932	-6	14	1.4	2836	-115	-82	0.6	1.1	
-3, 3/2, 0	sc	2523	-7	21	0.1	1.3	2512	0	1	-	2512	0	1	0.0	-	2511($\Sigma\Xi$)
	cc	2534	-10	23	0.1	1.2	2519	-87	8	0.7	2527	-8	15	0.1	1.4	
-3, 3/2, 1	sc	2514	0	3	0.0	-	2514	0	3	-	2527	-23	16	0.2	1.1	2703($\Xi\Sigma^*$)
	cc	2538	-6	27	0.1	1.2	2558	-49	47	0.7	2527	-23	16	0.2	1.1	
-3, 3/2, 2	sc	2707	0	4	0.0	-	2709	0	6	-	2699	-57	-3	0.6	0.9	2651($\Xi\Sigma\pi$)
	cc	2713	-26	10	0.1	1.1	2726	-45	23	0.8	2683	-63	-19	0.4	1.0	
-3, 3/2, 3	sc	2917	-11	13	0.1	1.3	2913	0	8	-	2766	-202	-152	1.0	0.9	2904($\Delta\Omega$)
	cc	2892	-54	-12	0.1	1.0	2934	-12	29	1.0	2754	-201	-150	1.0	0.9	
-6, 0, 0	sc	3334	-40	-11	0.1	1.1	3282	-281	-62	0.4	3350	-30	5	0.1	1.0	3345($\Omega\Omega$)
-6, 0, 1	sc	3355	-11	10	0.1	1.3	3323	-118	-21	0.6	3348	0	4	0.0	3.1	
-6, 0, 2	sc	3351	0	6	0.0	-	3358	-11	13	1.2	3346	0	1	0.0	-	
-6, 0, 3	sc	3346	0	1	0.0	-	3346	0	1	-	3346	0	1	1.0	-	

Table VII: The same as Table III for $S = -4, -5$.

Table VII		GBE(b)					FN				QDCSM					Threshold
SIJ		E_α	V_0	B_α	ϵ	R_s	E_α	V_0	B_α	R_s	E_α	V_0	B_α	ϵ	R_s	
-4, 0, 0	sc	2654	-5	18	0.0	1.4	2641	-39	5	1.0	2643	-24	7	0.1	1.2	2636($\Xi\Xi$)
	cc	2654	-5	18	0.0	1.4	2641	-40	5	1.0	2643	-24	7	0.1	1.2	
-4, 0, 1	sc	2806	-4	18	0.0	1.4	2793	-38	5	1.0	2796	-18	8	0.1	1.3	2788($\Lambda\Omega$)
	cc	2665	-26	29	0.1	0.9	2641	-118	5	0.6	3016	-113	380	1.0	0.3	
-4, 0, 2	sc	2789	0	1	0.0	-	2789	0	1	-	2789	0	1	0.0	-	
	cc	2789	0	1	0.0	-	2820	-4	32	1.1	2828	-50	40	1.0	0.7	
-4, 0, 3	sc	3073	-1	6	0.0	2.4	3072	0	5	-	3071	-11	4	0.2	1.6	3066($\Xi^*\Xi^*$)
-4, 1, 0	sc	2653	-3	17	0.0	1.5	2666	-93	30	0.6	2659	-3	23	0.1	1.3	2636($\Xi\Xi$)
	cc	2655	-4	19	0.0	1.4	2664	-95	28	0.6	2659	-4	23	0.1	1.3	
-4, 1, 1	sc	2637	0	1	0.0	-	2643	0	7	-	2637	0	1	0.0	-	
	cc	2637	0	1	0.0	-	2742	-17	106	0.6	2637	0	1	0.0	-	
-4, 1, 2	sc	2852	0	1	0.0	-	2852	0	1	-	2852	0	1	0.0	-	2851($\Xi\Xi^*$)
	cc	2873	-13	21	0.1	1.1	2893	-43	41	0.7	2862	-74	10	1.0	0.7	
-4, 1, 3	sc	3063	0	6	0.0	-	3061	0	4	-	2999	-96	-58	0.8	1.0	3057($\Sigma^*\Omega$)
	cc	3068	-12	11	0.1	1.3	3073	-3	16	1.4	3011	-84	-46	0.6	1.0	
-5, 1/2, 0	sc	3207	0	1	0.0	-	3100	-252	-106	0.5	3199	-37	-6	0.2	1.1	3205($\Xi^*\Omega$)
	cc	3213	0	7	0.0	-	3100	-252	-106	0.5	3199	-37	-6	0.2	1.1	
-5, 1/2, 1	sc	3001	-7	16	0.1	1.3	2977	-63	-14	0.9	3007	-7	17	0.1	1.3	2990($\Xi\Omega$)
	cc	3013	-10	22	0.1	1.1	3013	-136	22	0.5	3125	-24	134	1.0	0.5	
-5, 1/2, 2	sc	2991	0	1	0.0	-	2991	0	1	-	2991	0	1	0.0	-	
	cc	2998	0	7	0.0	-	3003	-3	13	1.6	2995	0	4	0.0	-	
-5, 1/2, 3	sc	3207	0	1	0.0	-	3207	0	1	-	3207	0	1	0.0	-	3205($\Xi^*\Omega$)
	cc	3213	0	7	0.0	-	3212	0	6	-	3216	-4	11	0.2	1.6	

FIGURE CAPTIONS

Fig.1 Channel coupling effect for GBE(a) and (b) where the state is denoted by the symbols S,I,J for spin, isospin and angular momentum. The single channel (sc) case for GBE(a) is shown as the solid curve; the channel coupling case (cc) for GBE(a) is shown as the thick solid curve; the single channel (sc) case for GBE(b) is shown as the dashed curve; the channel coupling case (cc) for GBE(b) is shown as the thick dashed curve.

Fig.2 The effect of different smearing forms for GBE models. The solid curve is for the GBE(a) model; the dashed curve is for the GBE(b) model.

Fig.3 Additional channels as in Fig.2

Fig.4 States with similar pure repulsive effective interactions for the GBE, FN and QDCSM models. The solid curve is for the QDCSM; the dashed curve is for the GBE model and the dotted curve is for the FN model.

Fig.5 The same as Fig.4 for states with similar weak attraction for all three models.

Fig.6 The same as Fig.4 for states with similar effective interactions for the QDCSM and FN models.

Fig.7 The same as Fig.4 for states with similar effective interactions for the QDCSM and GBE models.

Fig.8 The same as Fig.4 for states with similar effective interactions for the GBE and FN models.

Fig.9 States with effective interactions in the QDCSM which lie between those of the GBE and FN model. The curves for each model are as in Fig.4.

Fig.10 States with strong intermediate-range attraction in the QDCSM, for which $|V_0|$ decreases with the increasing strangeness. The curves for each models are as in Fig.4.

Fig.11 States for which $|V_0|$ increases with the increasing strangeness for the FN model. The curves for the models are as in Fig.1.

Fig.12 H particle with single channel and channel coupling in the QDCSM, GBE and FN models. The curves for the models are as in Fig.4, and the thick curves are for the channel coupling case.

FIG.1

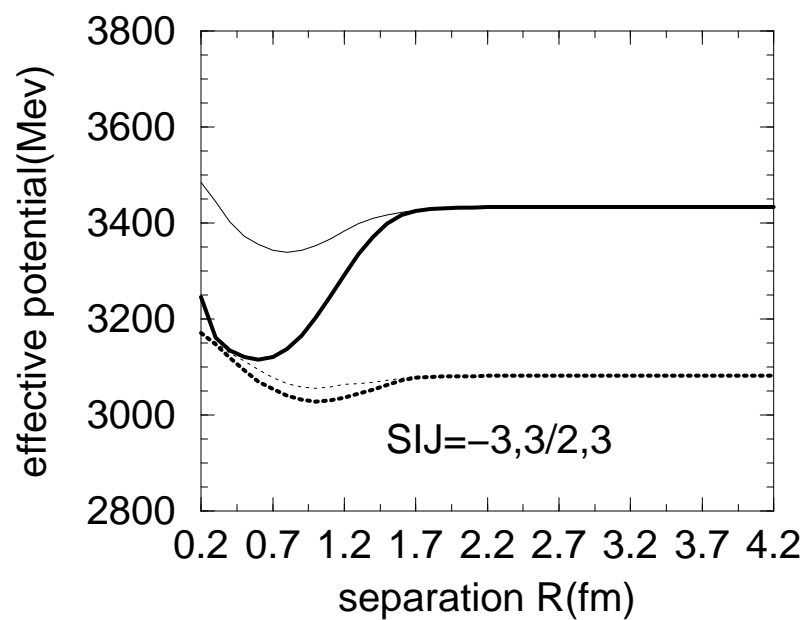
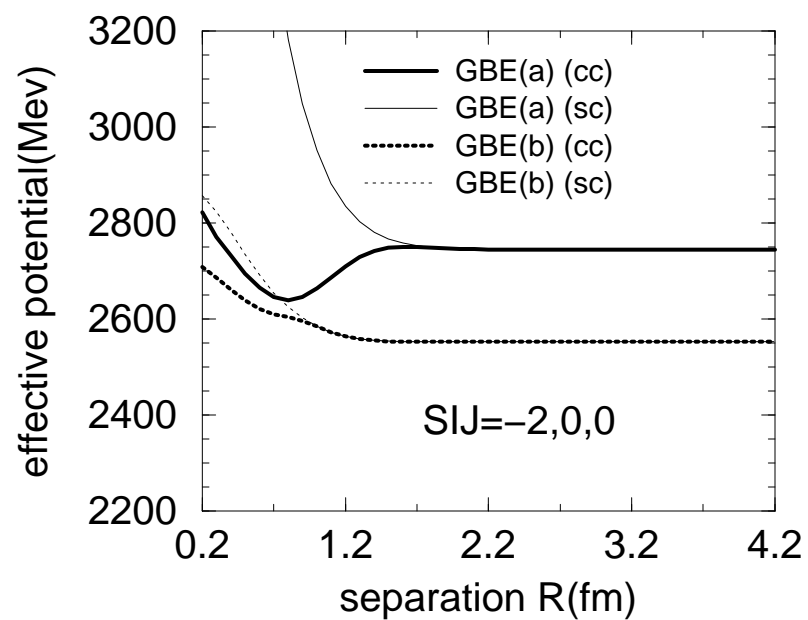


FIG.2

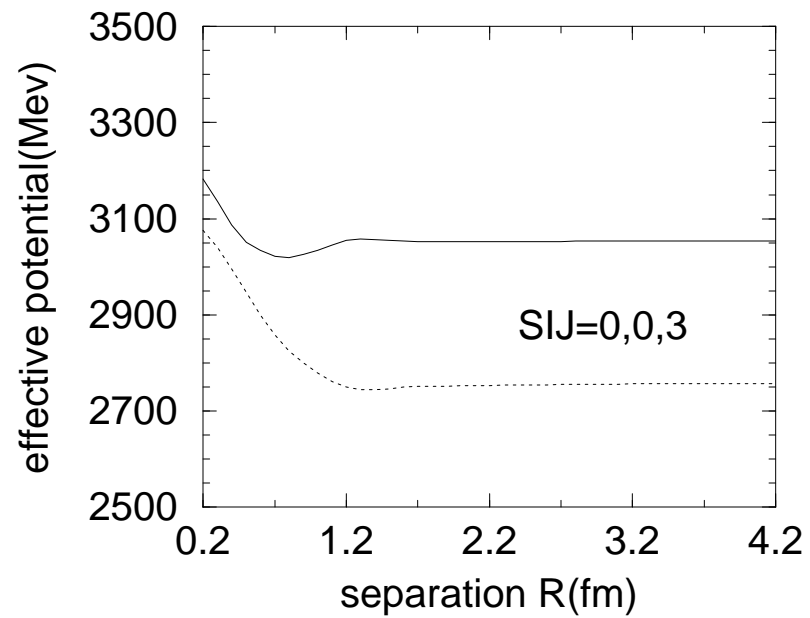
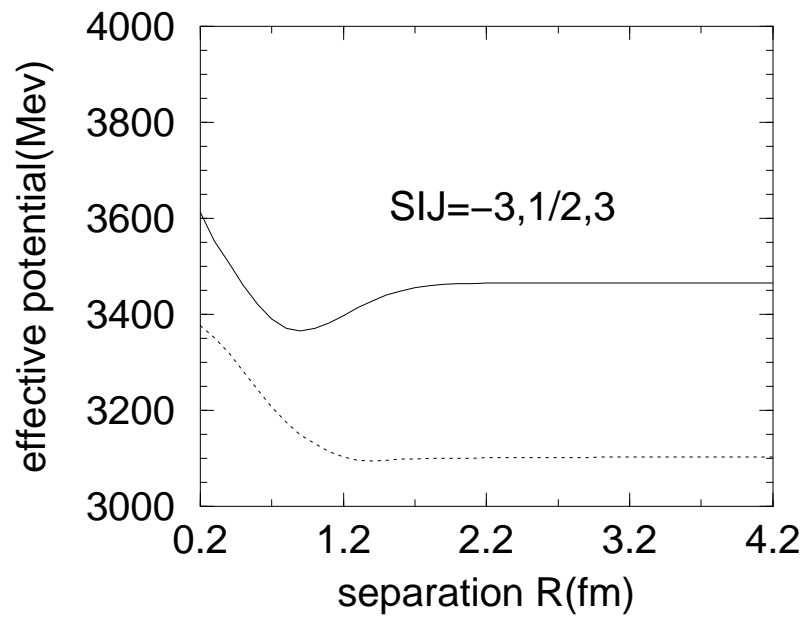
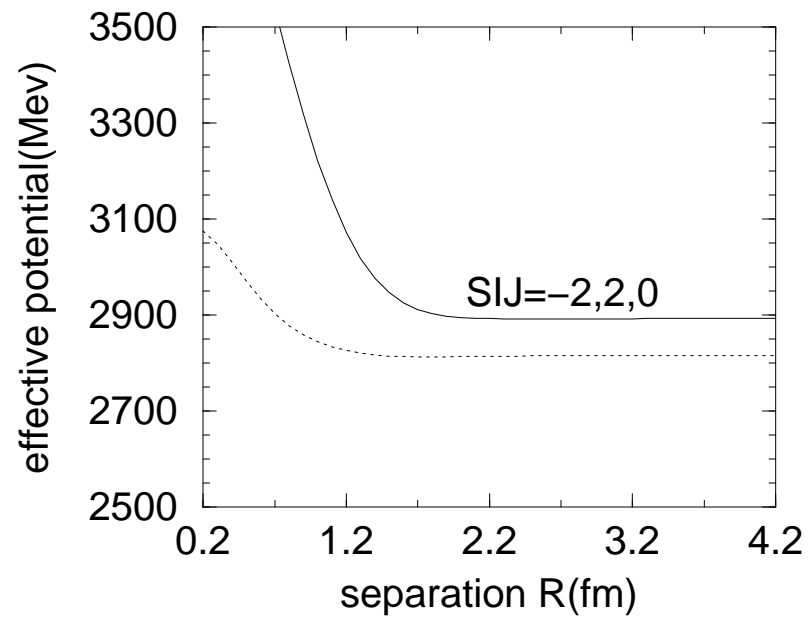
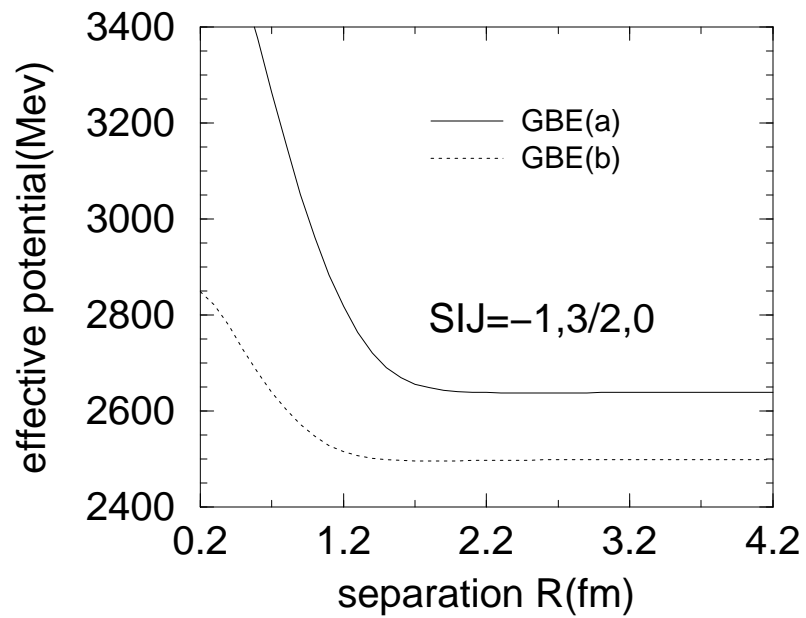


FIG.3

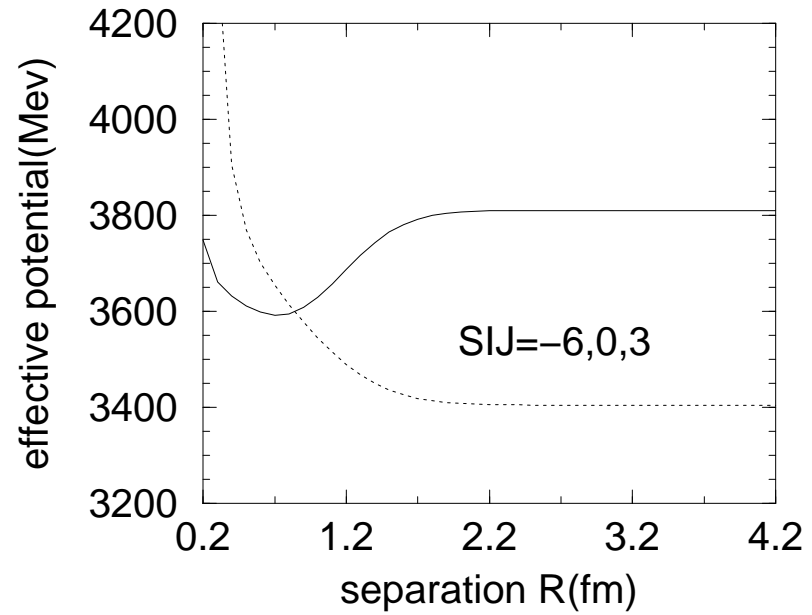
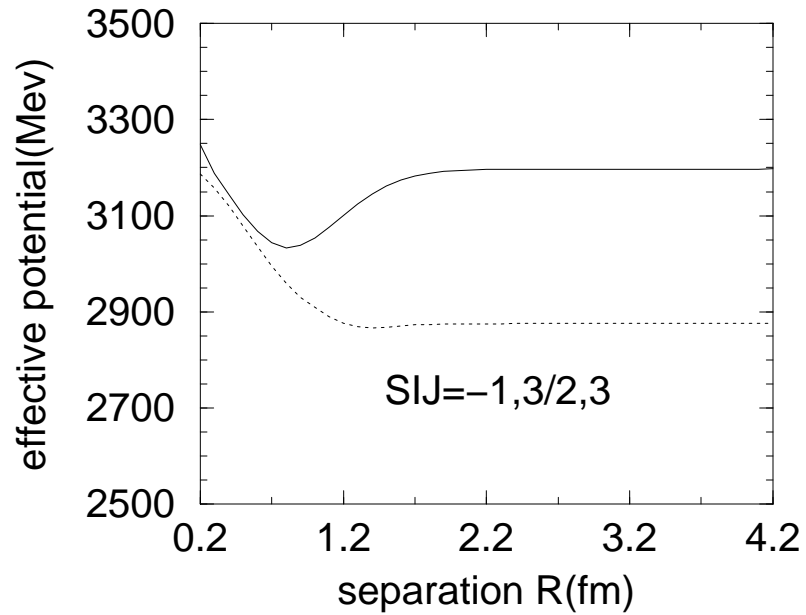
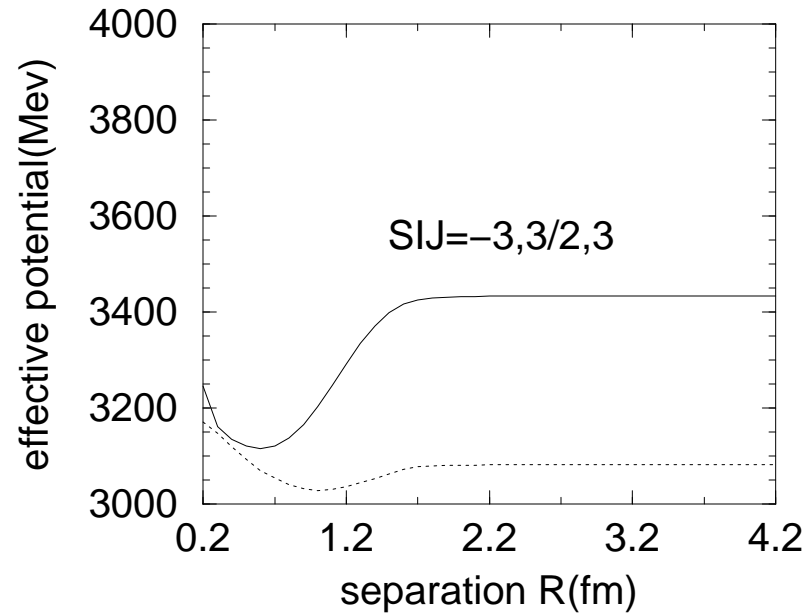
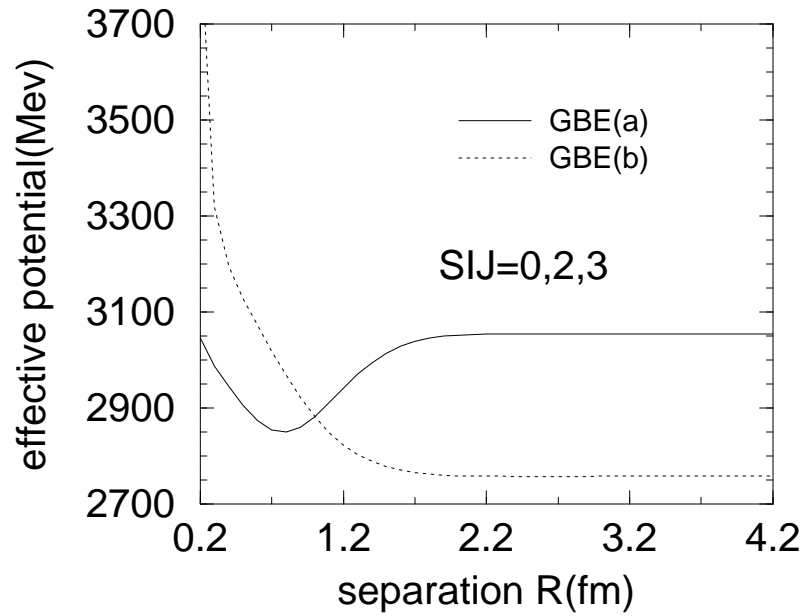


FIG.4

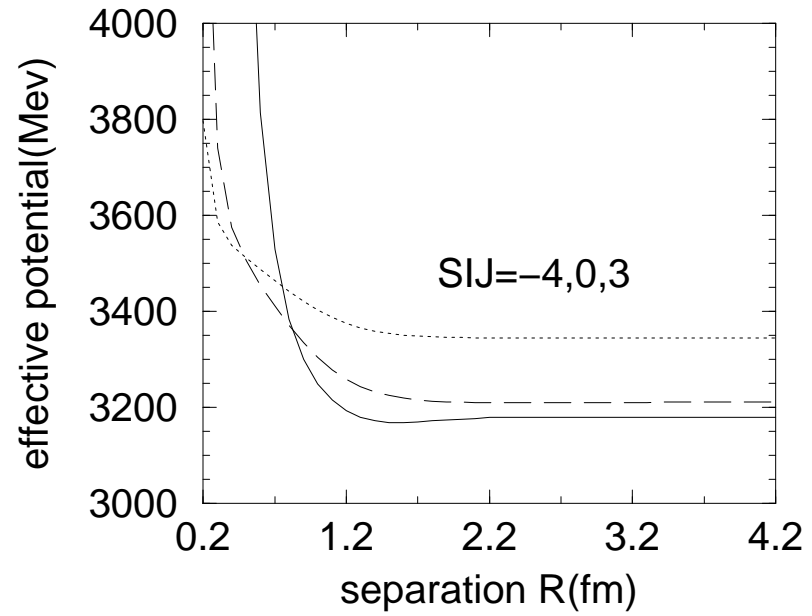
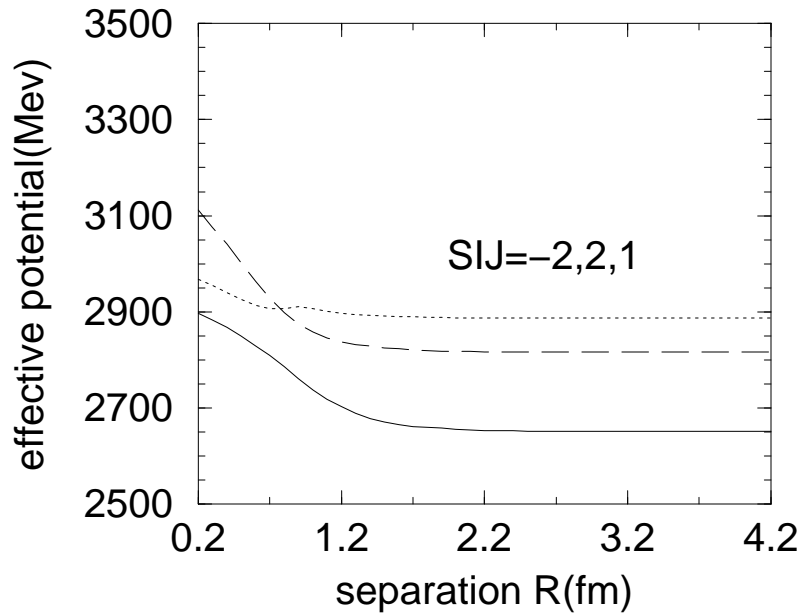
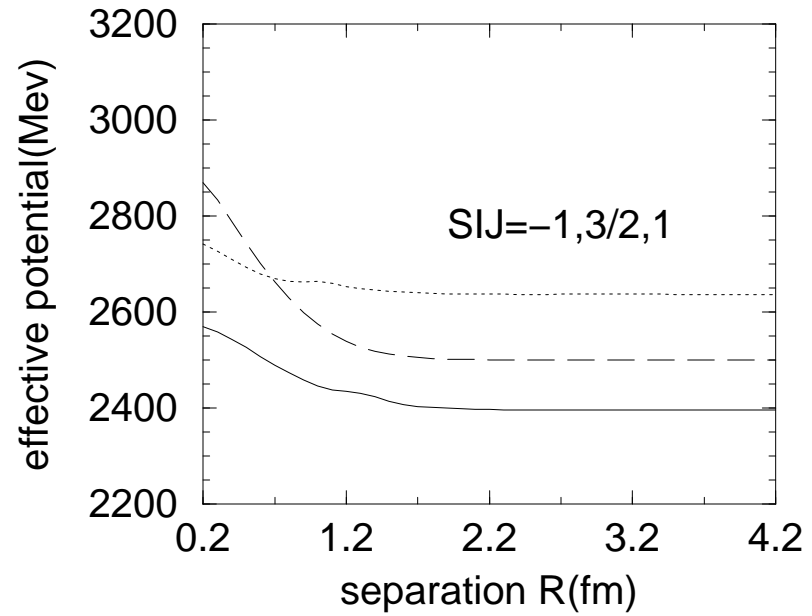
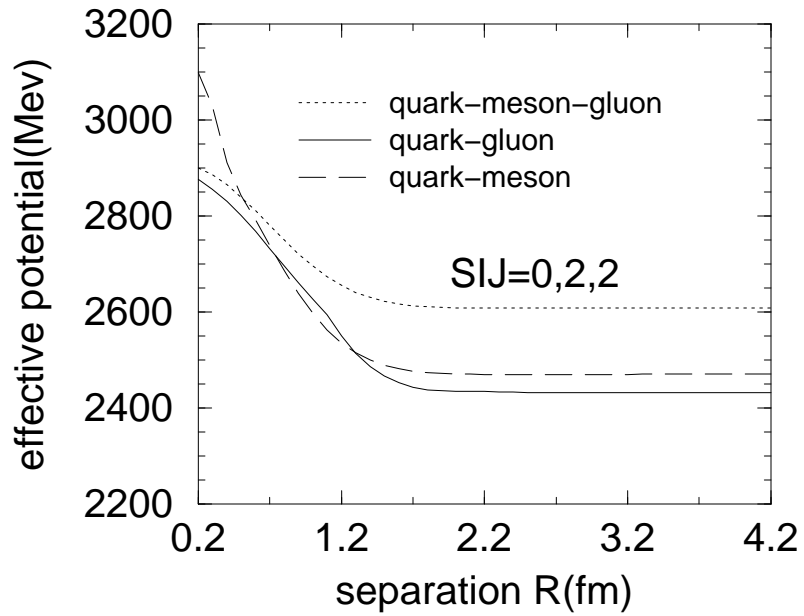


FIG.5

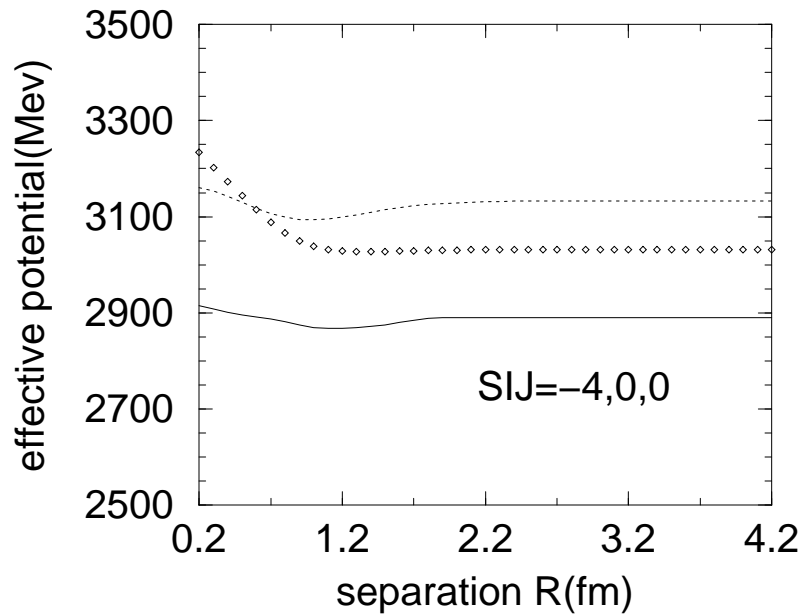
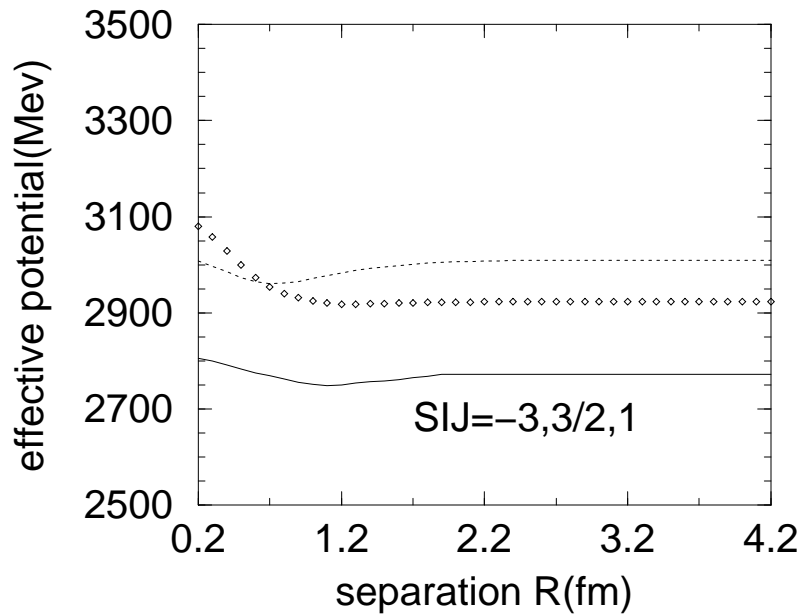
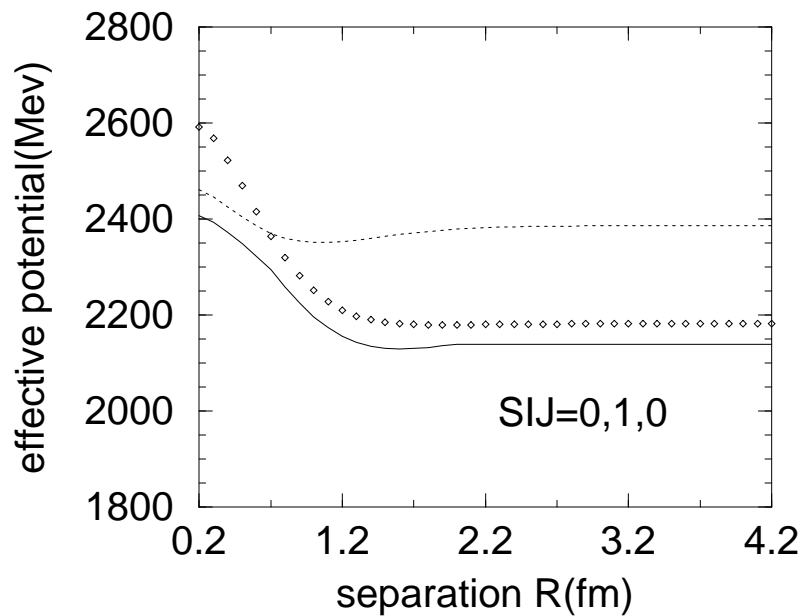
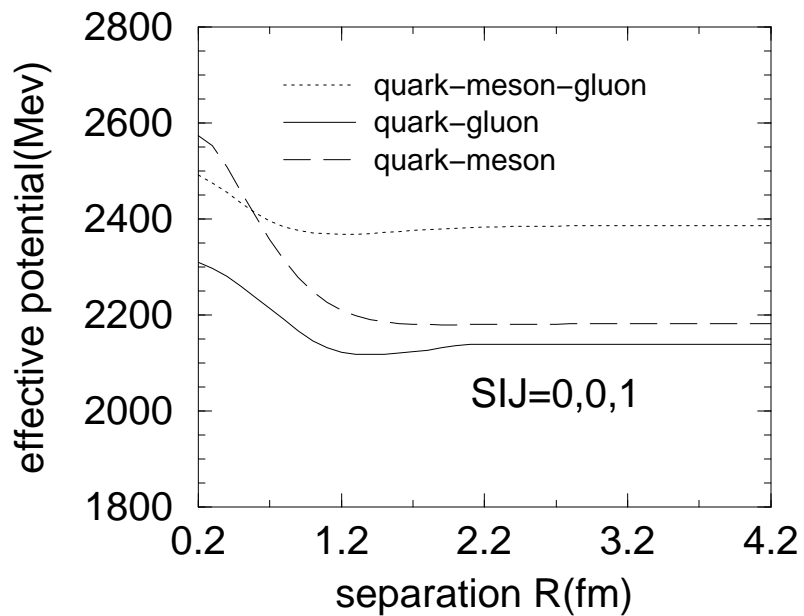


FIG.6

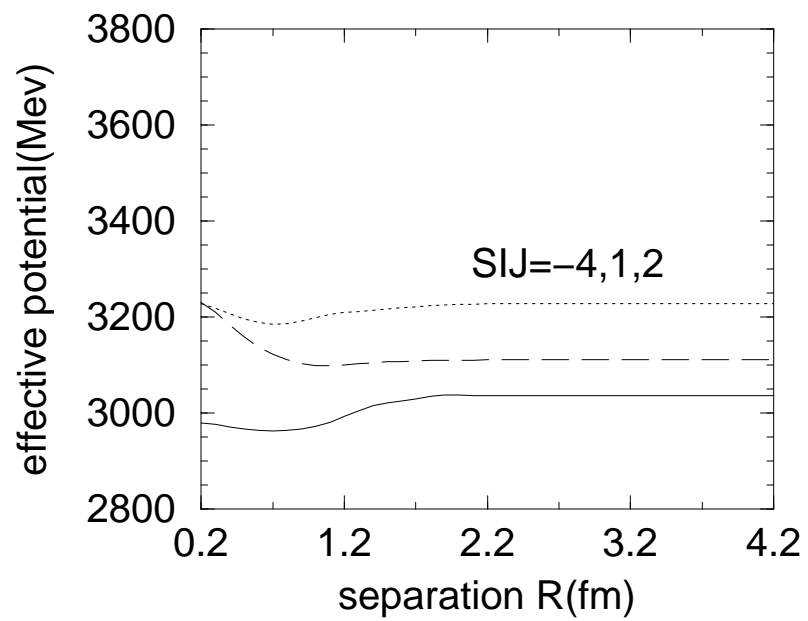
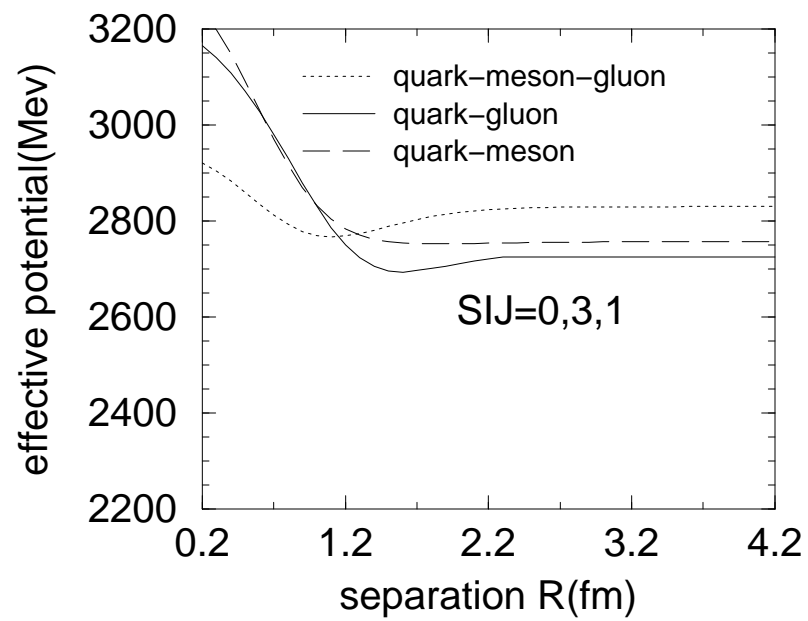


FIG.7

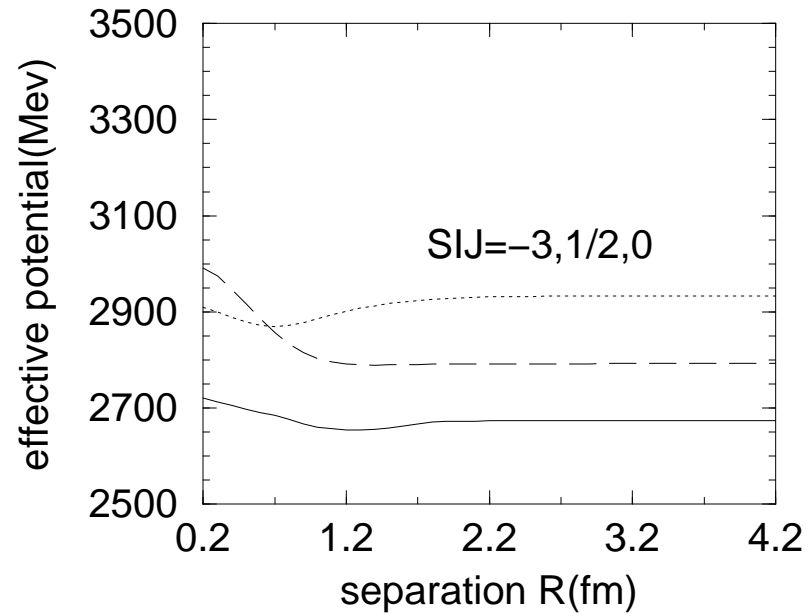
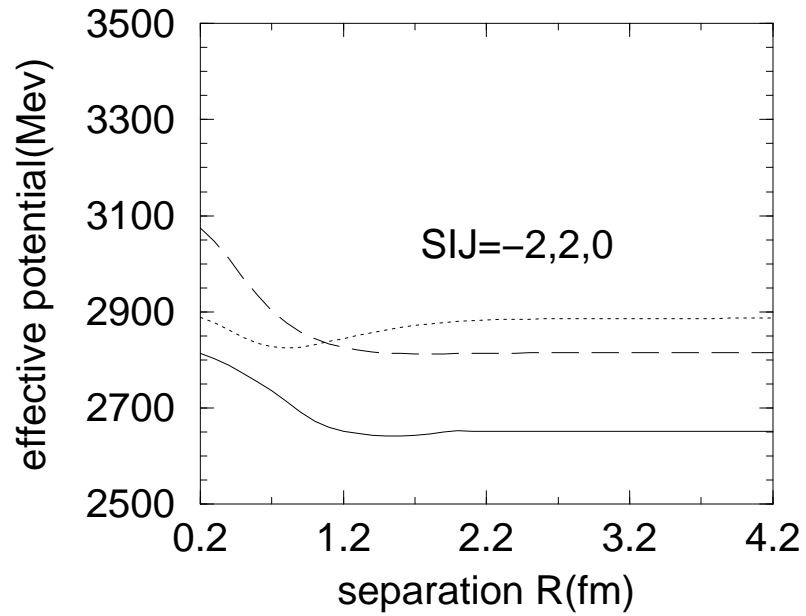
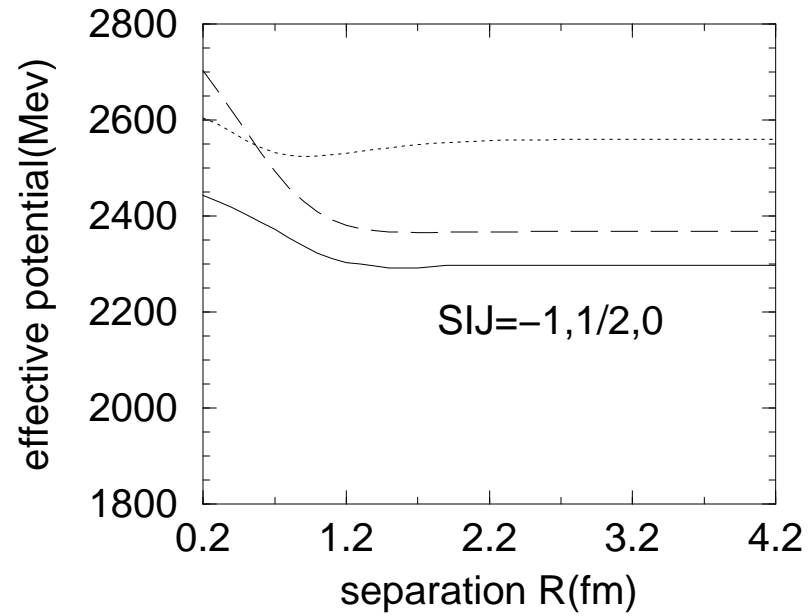
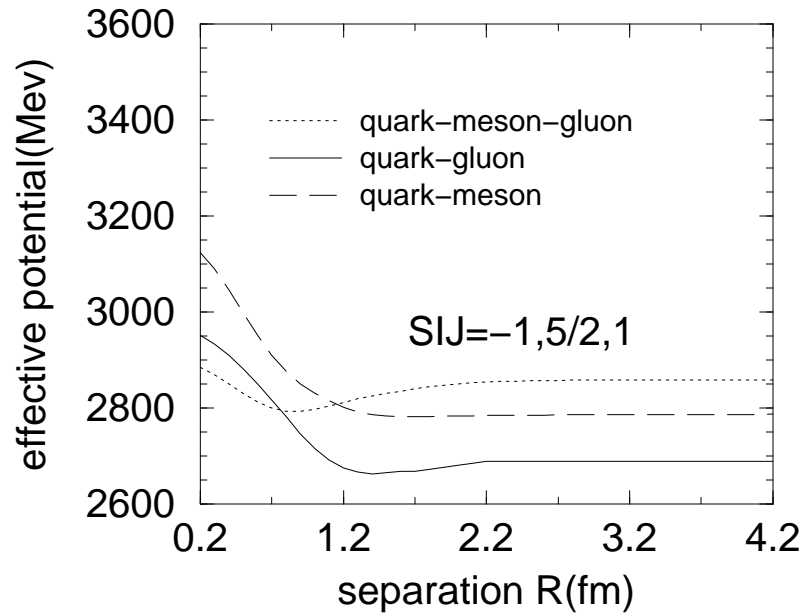


FIG.8

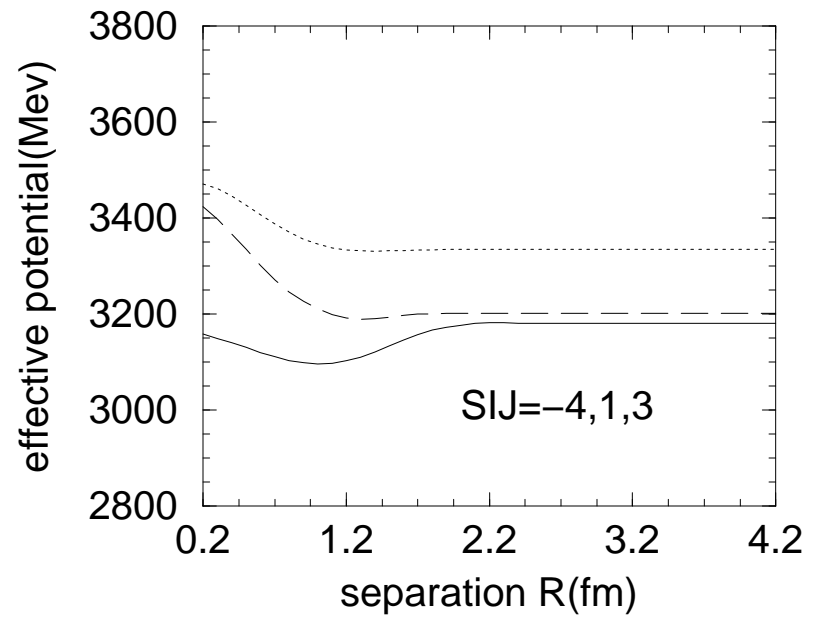
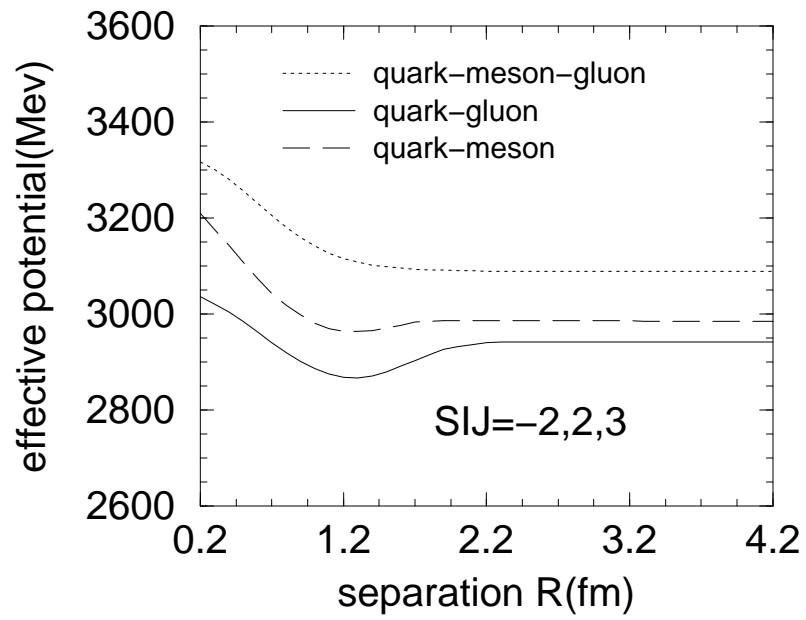


FIG.9

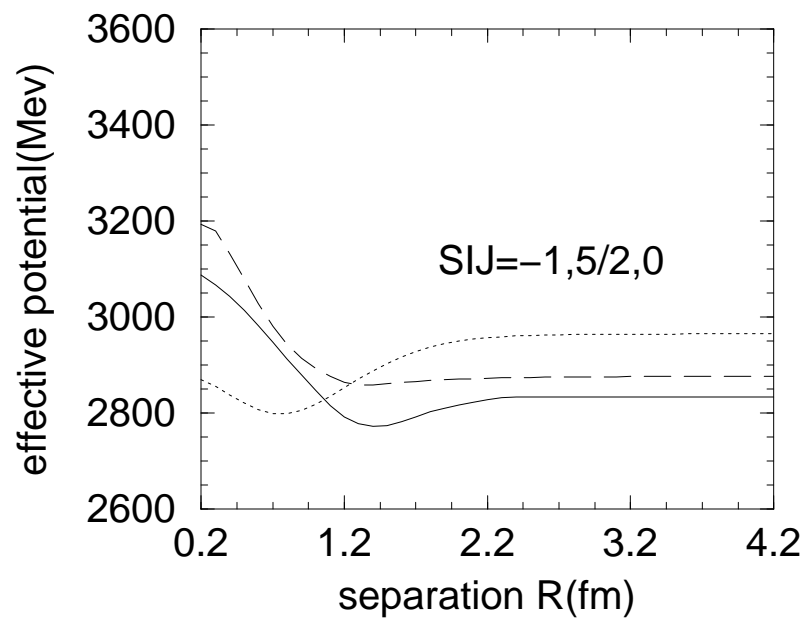
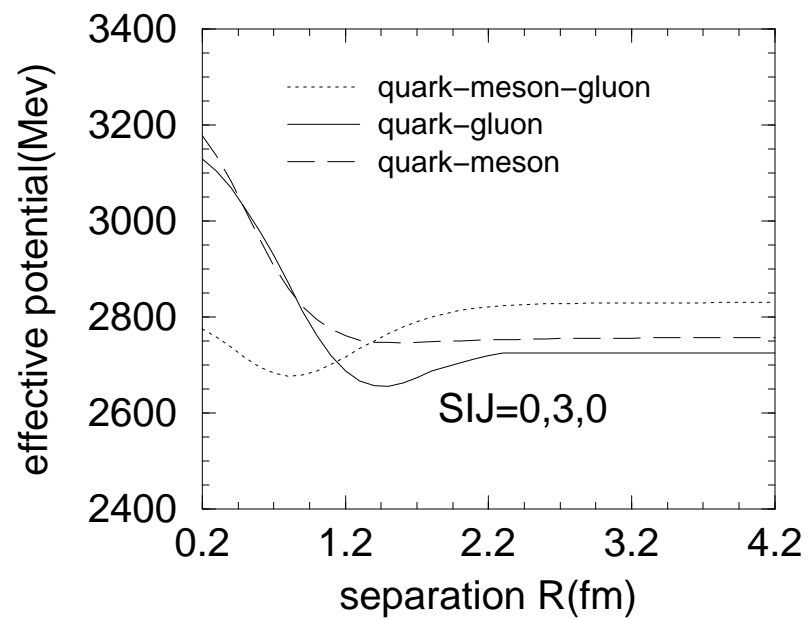


FIG.10

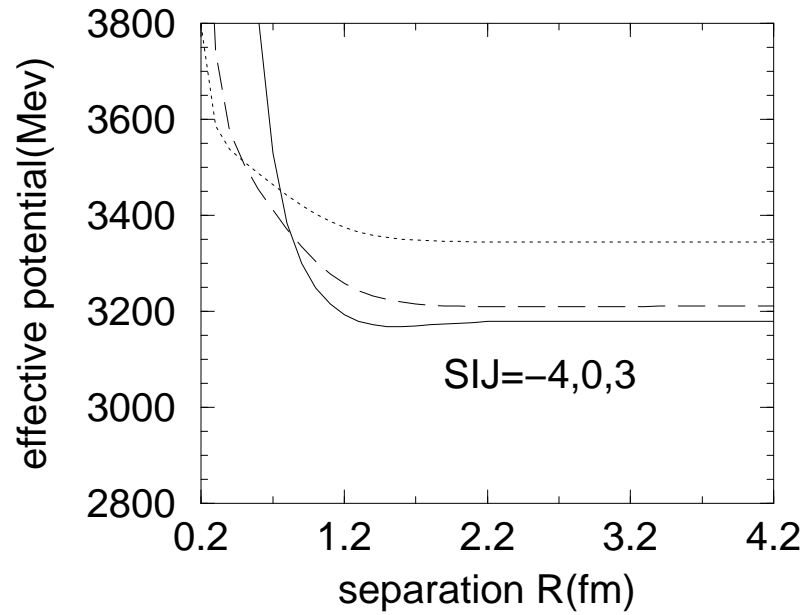
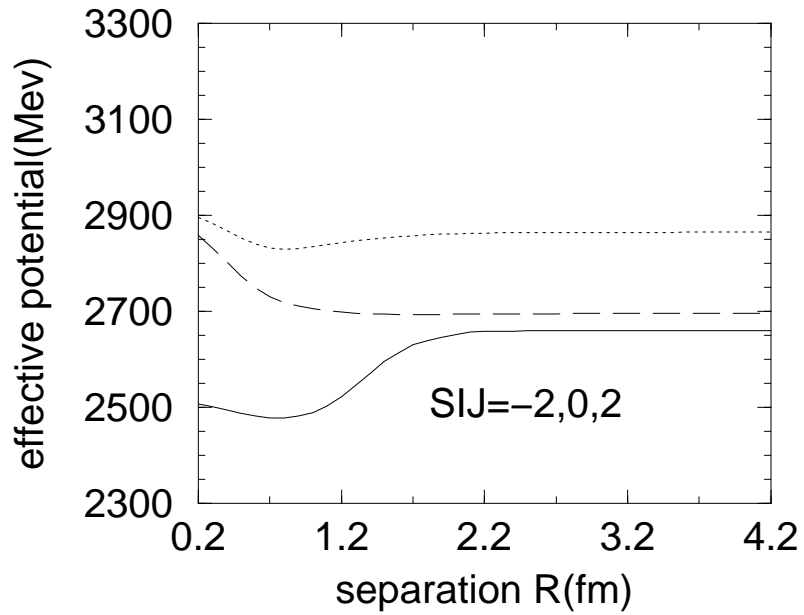
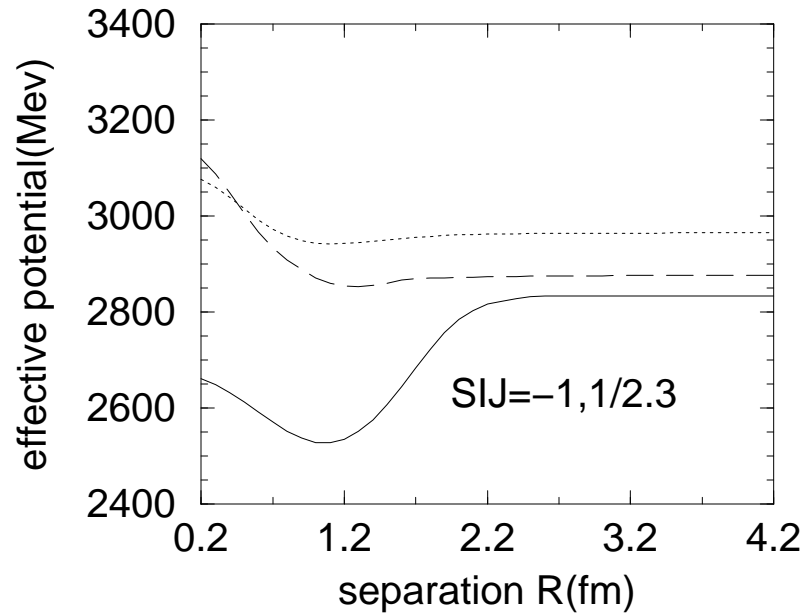
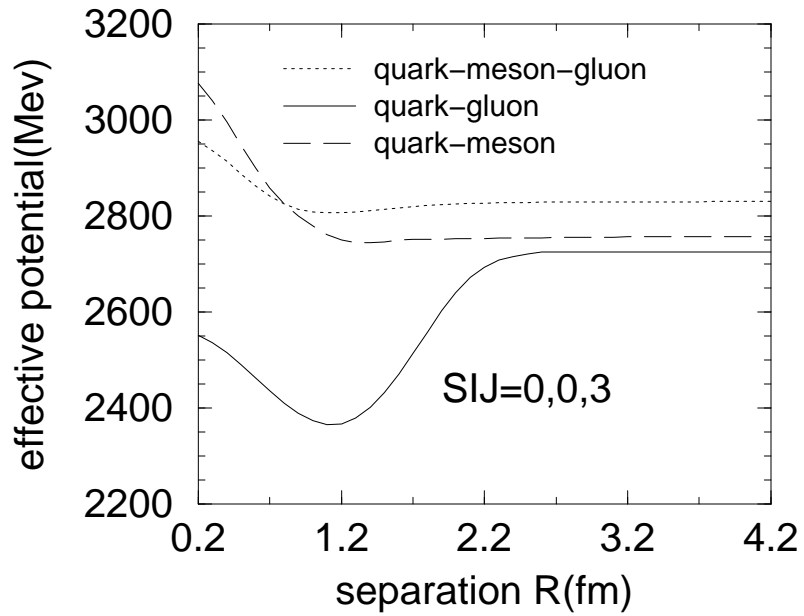


FIG.11

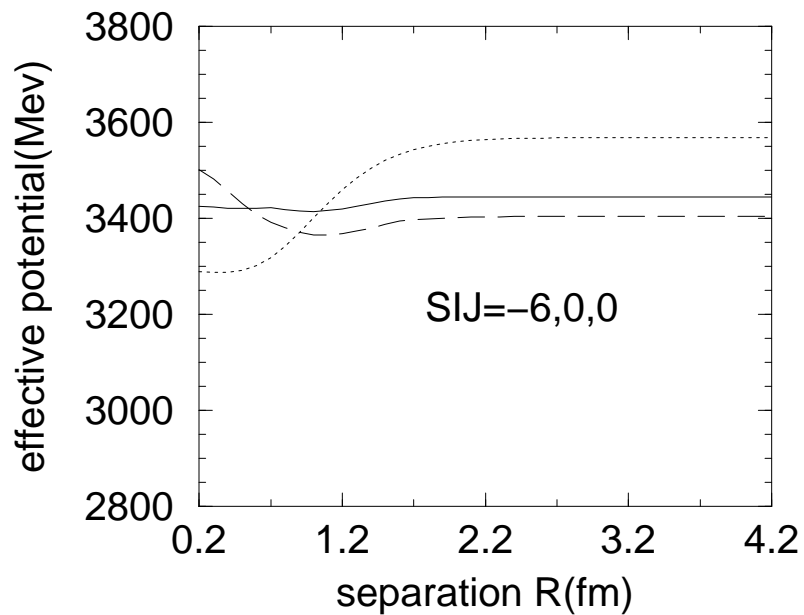
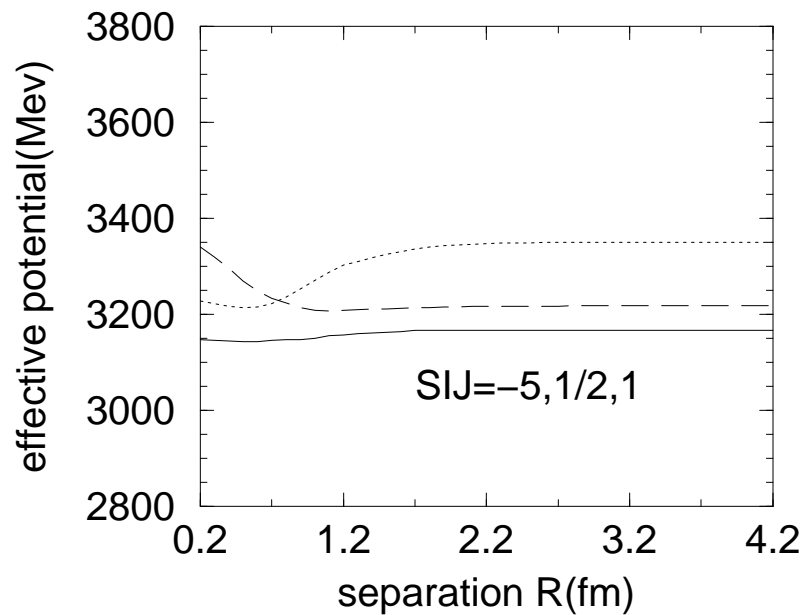
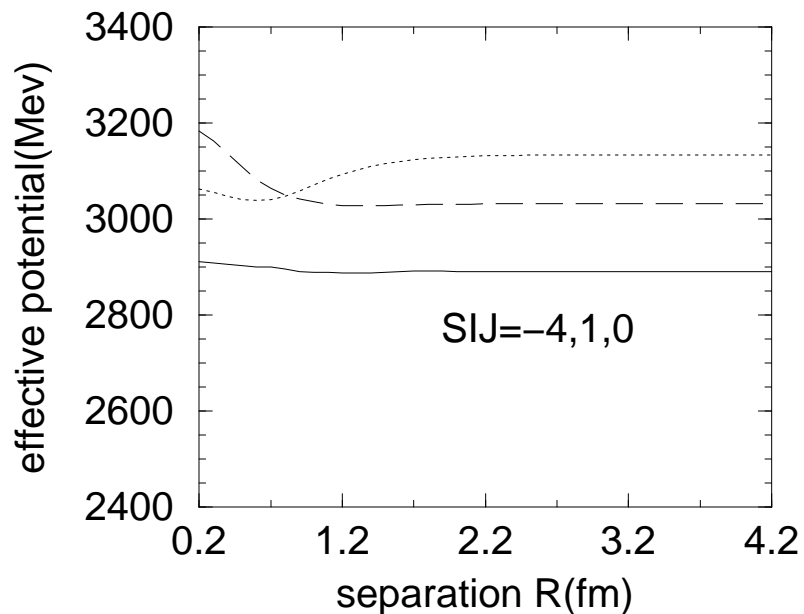
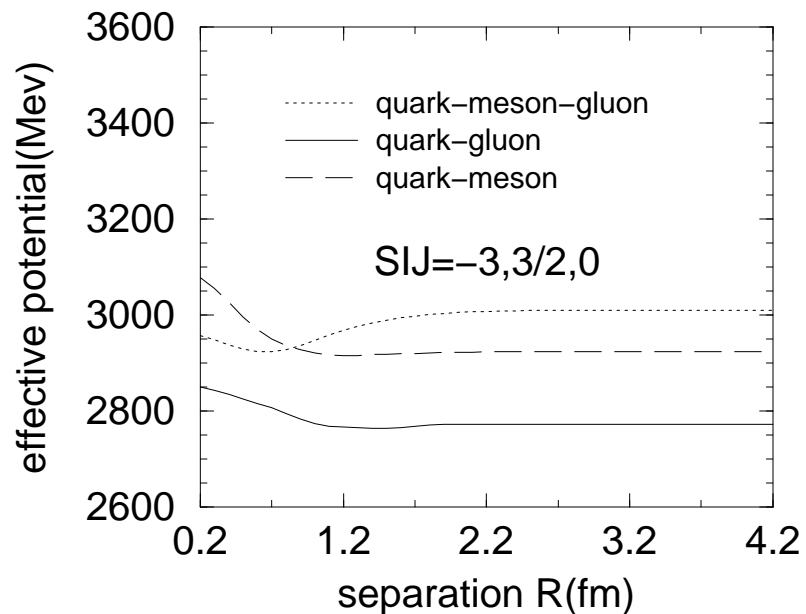


FIG.12

- quark-meson-gluon (cc)
- quark-gluon (cc)
- - - - quark-meson(b) (cc)
- quark-meson-gluon (sc)
- quark-gluon (sc)
- - - - quark-meson(b) (sc)

- quark-meson-gluon (cc)
- quark-gluon (cc)
- - - - quark-meson(a) (cc)
- quark-meson-gluon (sc)
- quark-gluon (sc)
- - - - quark-meson(a) (sc)

